

# Flavor and CP-violating Higgs sector in two Higgs doublet models with $U(1)'$

Ligong Bian<sup>1,\*</sup>, Hyun Min Lee<sup>2,†</sup> and Chan Beom Park<sup>3,‡</sup>

<sup>1</sup>*Department of Physics, Chongqing University, Chongqing 401331, China*

<sup>2</sup>*Department of Physics, Chung-Ang University, Seoul 06974, Korea*

<sup>3</sup>*Center for Theoretical Physics of the Universe,  
Institute for Basic Science (IBS), Daejeon 34126, Korea*

## Abstract

We investigate the role of a local  $U(1)'$  symmetry for the problem of CP violation in the effective theory for two Higgs doublet models and its microscopic counterparts. First, in two Higgs doublet models with  $U(1)'$ , we show that the higher-dimensional operators in the scalar potential violate the CP symmetry with an interplay with the mixing mass parameter, giving rise to small mixings between CP-even and CP-odd scalars. Motivated by the  $B$ -meson anomalies in recent years, we take the flavored  $U(1)'$  to be a benchmark model for specifying the flavor structure. Then, we calculate the electric dipole moment of electron (eEDM) at two loops due to the CP-violating higher-dimensional operators and identify the correlation between the masses of heavy Higgs bosons and the cutoff scale from the bound on eEDM. We also comment on the possibility of making an independent test of the CP violation in the collider searches for heavy Higgs bosons. Finally, we show how the obtained eEDM results in the effective theory can be used to constrain microscopic models with an explicit CP violation in the partially decoupled or dark sectors.

\*Email: lgbycl@cqu.edu.cn

†Email: hminlee@cau.ac.kr

‡Email: cbpark@ibs.re.kr

# 1 Introduction

It is an important task to understand the flavor structure of the Standard Model (SM) and the origin of CP violation, calling for physics beyond the SM. In particular, a violation of lepton flavor universality would be an important indirect test of the SM, and it provides a guideline for going beyond the SM and designing the high energy colliders in the next generations beyond the Large Hadron Collider (LHC). We also need to look for the source of a new CP violation beyond the SM in order to explain the matter-antimatter asymmetry in the Universe.

In models with an extended Higgs sector, we may have new sources for the CP violation unless CP is conserved by a symmetry argument or ansatz [1]. One of the most stringent constraints on the CP violation is from the electric dipole moment (EDM) of the electron and the neutron counterparts. Thus, we need to find a way to make a sufficient suppression of the new physics contributions of new CP phases to the EDMs. In this regard, an extra  $U(1)'$  symmetry plays an important role in controlling the CP violation, at least, in the Higgs sector, because it protects the CP symmetry from being broken at the renormalizable level in two Higgs doublet models (2HDMs).

In recent years, there have been interesting anomalies in the semi-leptonic decays of  $B$ -mesons, hinting at the violation of lepton flavor universality in the SM with about  $2-3\sigma$  deviation at each observable. The measured values of  $R_K = \mathcal{B}(B \rightarrow K\mu^+\mu^-)/\mathcal{B}(B \rightarrow Ke^+e^-)$  from LHCb data [2, 3] as well as the similar ratio for vector  $B$ -mesons,  $R_{K^*} = \mathcal{B}(B \rightarrow K^*\mu^+\mu^-)/\mathcal{B}(B \rightarrow K^*e^+e^-)$  from LHCb [4], show deviations from the SM predictions. The deviation in  $R_{K^*}$  is supported by the reduction in the angular distribution of  $B \rightarrow K^*\mu^+\mu^-$  [5]. The recent update on  $R_{K^*}$  from Belle data [6] shows a similar deviation in low energy bins, although the combined fits in high energy bins in Belle [7] are consistent with the SM but with large error bars. As a result, the combined significance for the global fits of the  $B$ -meson data turns out to be about  $5-6\sigma$  [8, 9].

The  $B$ -meson anomalies can be accounted for by the introduction of a flavor-dependent  $U(1)'$  distinguishing between leptons in the SM [10, 11]. But, the flavor  $U(1)'$  necessarily requires at least two Higgs doublets, and it gives rise to flavor-violating couplings for the  $Z'$  gauge boson and new Higgs bosons [11]. As a consequence, there are testable signatures of the flavor-dependent  $U(1)'$  from other  $B$ -meson decays and mixings, as well as flavor-violating productions and decays of heavy Higgs bosons at the LHC [11]. However, in this class of models with flavored  $U(1)'$ , the CP symmetry is well protected at the renormalizable level.

In this article, taking a flavor-dependent  $U(1)'$  as a benchmark model in Refs. [10, 11] to explain the  $B$ -meson anomalies, we undertake a concrete discussion on the problem of CP violation in the 2HDM. We investigate the salient features of the CP-violating Higgs sector in the effective theory, that are applicable to general 2HDMs with  $U(1)'$  beyond any flavor-specific  $U(1)'$ . Including higher-dimensional operators with extra CP phases in the Higgs potential, we show that the mixing mass parameter in the Higgs potential gets a nontrivial CP phase by the tadpole condition, resulting in the mixings between CP-even and

CP-odd neutral scalars in the model. Taking into account the contribution of the new CP phase to the electric dipole moment of the electron, we correlate between heavy Higgs boson masses and new physics scales for the higher-dimensional operators. We also address the implications of the Higgs mixings for the collider searches of CP-violating Higgs resonances and present some microscopic  $U(1)'$  models with extra matter content for generating the higher dimensional operators with new CP phases in the Higgs potential.

The rest of the paper is organized as follows. We begin with a description of the Higgs potential in two Higgs doublet models with a local  $U(1)'$  and take the  $U(1)'$  to be flavor-dependent for the specific Yukawa couplings for the SM fermions. Then, we study the tadpole conditions from the minimization of the potential in the presence of the  $U(1)'$  invariant higher-dimensional operators up to dimension-6 and derive the mixings between neutral scalars of the model and the CP-violating Yukawa couplings to SM quarks and leptons. Next, we update the constraints on the  $Z'$  mass and couplings from  $B$ -meson anomalies and calculate the electric dipole moments from the Higgs mixings. We also comment on the anomalous magnetic dipole moment of leptons and the collider searches for CP-violating resonance searches for extra Higgs bosons. We continue to provide the  $U(1)'$  Next-to-Minimal Supersymmetric Standard Model (NMSSM) and the  $U(1)'$  models with extra doublet and singlet scalars or fermions as the microscopic origin of the higher dimensional operators with nontrivial CP phases. Finally, conclusions are drawn. There are three appendices, dealing with the minimization conditions, the diagonalization of scalar mass matrices, and the self-interactions and gauge interactions of scalar fields.

## 2 Two Higgs doublet models with local $U(1)'$

In models with a local  $U(1)'$  under which two Higgs doublets carry nonzero charges, we consider the CP symmetry in the scalar potential and describe the flavored  $U(1)'$  for a concrete discussion on the Yukawa structure in this model.

### 2.1 The scalar potential with $U(1)'$

We introduce an extra  $U(1)'$  with flavor-dependent charges beyond the SM. Then, it is necessary to introduce at least two Higgs doublet,  $H_1$  and  $H_2$ , either of which carries a nonzero  $U(1)'$  charge. We also need to introduce a complex singlet scalar  $S$  to break the  $U(1)'$  symmetry spontaneously and allow for a correct electroweak symmetry breaking. As a result, in terms of the primed notations for scalar fields and their couplings for convenience in the later discussion, the renormalizable scalar potential is given by

$$\begin{aligned}
 V_1 = & \mu_1'^2 |H_1'|^2 + \mu_2'^2 |H_2'|^2 - \left( \mu' S H_1'^\dagger H_2' + \text{h.c.} \right) \\
 & + \lambda_1' |H_1'|^4 + \lambda_2' |H_2'|^4 + 2\lambda_3 |H_1'|^2 |H_2'|^2 + 2\lambda_4' (H_1'^\dagger H_2') (H_2'^\dagger H_1') \\
 & + 2|S'|^2 (\kappa_1' |H_1'|^2 + \kappa_2' |H_2'|^2) + m_S'^2 |S'|^2 + \lambda_S' |S'|^4.
 \end{aligned} \tag{2.1}$$

Therefore, according to the results on the tadpole conditions shown in Appendix A, the extra CP phase coming from  $\mu'$  is set to zero, so the CP symmetry is protected at the renormalization level. The consequence generally holds for the 2HDMs where the Higgs doublets carry nonzero  $U(1)'$  charges, irrespective of whether the  $U(1)'$  symmetry is flavor-dependent or not. However, the CP symmetry is an accidental symmetry at the renormalizable level, so the inclusion of higher-dimensional operators in the scalar potential generically gives rise to nonzero CP phases, which may not be set to zero by the tadpole conditions.

In the next subsection, we take the  $U(1)'$  to couple to the SM fermions in a flavor-dependent way, with a motivation to explain the  $B$ -meson anomalies at the LHCb. In this case, we can also determine the Yukawa couplings with flavor-dependent  $U(1)'$  charges taken into account, so make a concrete discussion of the CP violation in the physical observables.

## 2.2 A concrete model for flavored $U(1)'$

For a concrete discussion on the violation of flavor and CP, we henceforth take a specific model for the flavored  $U(1)'$ . Nonetheless, our following discussion on the CP-violating Higgs still holds for general two Higgs doublet models with  $U(1)'$ , under which either of two Higgs doublets carries a nonzero charge.

We regard the new gauge boson  $Z'$  associated with the  $U(1)'$  symmetry to couple specifically to heavy flavors as a linear combination of  $U(1)_{L_\mu-L_\tau}$  and  $U(1)_{B_3-L_3}$ , proposed in Refs. [10, 11], as follows.

$$Q' \equiv y(L_\mu - L_\tau) + x(B_3 - L_3),$$

where  $x$  and  $y$  are real parameters. Only the ratio of the  $x$  and  $y$  parameters is physically meaningful as either of them is absorbed by the  $Z'$  gauge coupling. Then, it is necessary to introduce two Higgs doublets  $H_{1,2}$  for obtaining correct quark masses and mixings [10, 11]. Moreover, in order to cancel the gauge anomalies, the fermion sector is required to include at least two right-handed neutrinos  $\nu_{iR}$  ( $i = 2, 3$ ). One more right-handed neutrino  $\nu_{1R}$  with zero  $U(1)'$  charge as well as extra singlet scalars,  $\Phi_a$  ( $a = 1, 2, 3$ ), with  $U(1)'$  charges of  $-y$ ,  $x + y$ ,  $x$ , respectively, are also necessary for neutrino masses and mixings. The  $U(1)'$  charge assignments are given in Table 1.

The Lagrangian of the model is given as

$$\mathcal{L} = -\frac{1}{4}Z'_{\mu\nu}Z'^{\mu\nu} - \frac{1}{2}\sin\xi Z'_{\mu\nu}B^{\mu\nu} + \mathcal{L}_S + \mathcal{L}_Y \quad (2.2)$$

with

$$\mathcal{L}_S = |D_\mu H_1|^2 + |D_\mu H_2|^2 + |D_\mu S|^2 + \sum_{a=1}^3 |D_\mu \Phi_a|^2 - V(\phi_i), \quad (2.3)$$

where  $Z'_{\mu\nu} = \partial_\mu Z'_\nu - \partial_\nu Z'_\mu$  is the field strength of the  $U(1)'$  gauge boson,  $\sin\xi$  is the gauge kinetic mixing between  $U(1)'$  and the SM hypercharge.  $D_\mu\phi_i = (\partial_\mu - ig_{Z'}Q'_{\phi_i}Z'_\mu)\phi_i$  are covariant derivatives. Here  $Q'_{\phi_i}$  is the  $U(1)'$  charge of  $\phi_i$ , and  $g_{Z'}$  is the extra gauge coupling.

	$q_{3L}$	$u_{3R}$	$d_{3R}$	$\ell_{2L}$	$e_{2R}$	$\nu_{2R}$	$\ell_{3L}$	$e_{3R}$	$\nu_{3R}$
$Q'$	$\frac{1}{3}x$	$\frac{1}{3}x$	$\frac{1}{3}x$	$y$	$y$	$y$	$-x-y$	$-x-y$	$-x-y$

	$S$	$H_1$	$H_2$	$\Phi_1$	$\Phi_2$	$\Phi_3$
$Q'$	$\frac{1}{3}x$	0	$-\frac{1}{3}x$	$-y$	$x+y$	$x$

Table 1:  $U(1)'$  charges of fermions and scalars.

The full scalar potential  $V(\phi_i)$  is composed of  $V = V_1 + V_2 + V_3$  with  $V_1$  given in Eq. (2.1), and  $V_2$  the renormalizable terms containing the extra singlet scalar fields,  $\Phi_a$ , as well as  $V_3$  being the higher dimensional operators, as follows,

$$\begin{aligned}
V_2 = & \sum_{a=1}^3 \left( \mu_{\Phi_a}^2 |\Phi'_a|^2 + \lambda'_{\Phi_a} |\Phi'_a|^4 \right) + \left( \rho' S^3 \Phi_3'^\dagger + \mu'_{\Phi} \Phi_1' \Phi_2' \Phi_3'^\dagger + \text{h.c.} \right) \\
& + 2 \sum_{a=1}^3 |\Phi'_a|^2 (\beta'_{a1} |H_1'|^2 + \beta'_{a2} |H_2'|^2 + \beta'_{a3} |S'|^2) + 2 \sum_{a<b} \lambda'_{ab} |\Phi'_a|^2 |\Phi'_b|^2, \tag{2.4}
\end{aligned}$$

$$V_3 = \frac{c'_1}{\Lambda^2} S'^2 (H_1'^\dagger H_2')^2 + \frac{c'_2}{\Lambda^2} S'^\dagger \Phi_3' (H_1'^\dagger H_2')^2 + \frac{d'_1}{\Lambda} S'^3 \Phi_1' \Phi_2' + \frac{d'_2}{\Lambda^2} (\Phi_1' \Phi_2' \Phi_3'^\dagger)^2 + \text{h.c.} + \dots \tag{2.5}$$

Here, we have kept up to dimension-6 terms in the potential  $V_3$  and the ellipses denote even higher dimensional terms. Then, there are new CP phases from  $\mu'$ ,  $\rho'$ ,  $\mu'_{\Phi}$  as well as  $c'_1$ ,  $c'_2$ ,  $c'_3$ ,  $d'_1$ ,  $d'_2$ , etc. We note that the dimension-6 operator,  $(S' H_1'^\dagger H_2')^2$ , always exists in general 2HDMs with  $U(1)'$  whereas the rest of higher-dimensional operators are model-dependent. In the later discussion on the CP violation, we will focus on  $(S' H_1'^\dagger H_2')^2$ .

For completeness and the concrete discussion on CP-violating Yukawa couplings to heavy Higgs bosons, we also introduce the  $U(1)'$  invariant Lagrangian for the Yukawa couplings for quarks and leptons, which is given by

$$\begin{aligned}
-\mathcal{L}_Y = & \bar{q}'_i (y'_{ij}{}^u \tilde{H}'_1 + h'_{ij}{}^u \tilde{H}'_2) u'_j + \bar{q}'_i (y'_{ij}{}^d H'_1 + h'_{ij}{}^d H'_2) d'_j \\
& + y'_{ij}{}^\ell \bar{\ell}'_i H'_1 e'_j + y'_{ij}{}^\nu \bar{\ell}'_i \tilde{H}'_1 \nu'_{jR} + \frac{1}{2} \overline{(\nu'_{iR})^c} (M_{ij} + z_{ij}^{(a)} \Phi'_a) \nu'_{jR} + \text{h.c.} \tag{2.6}
\end{aligned}$$

with  $\tilde{H}'_{1,2} \equiv i\sigma_2 H'^{*}_{1,2}$ .

### 3 CP violation in the Higgs sector

Considering the higher-dimensional terms in the effective scalar potential in the benchmark models with flavored  $U(1)'$  in the previous section, we discuss the Higgs spectrum and the

mixings between CP-even and CP-odd scalars.

### 3.1 Scalar mass matrix with CP violation

In unitary gauge, the Higgs doublet and singlet fields including the CP phases can be expressed by

$$\begin{aligned}
H'_j &= e^{i\theta_j} \begin{pmatrix} \phi_j^\dagger \\ (v_j + \rho_j + i\eta_j)/\sqrt{2} \end{pmatrix}, \quad (j = 1, 2), \\
S' &= \frac{1}{\sqrt{2}} e^{i\theta_S} (v_s + S_R + iS_I), \\
\Phi'_a &= \frac{1}{\sqrt{2}} e^{i\xi_a} (\omega_a + \Phi_{aR} + i\Phi_{aI}), \quad (a = 1, 2, 3).
\end{aligned} \tag{3.1}$$

We can always make the phase rotations to make all the vacuum expectation values (VEVs) real as follows:

$$H_j = e^{-i\theta_j} H'_j, \tag{3.2}$$

$$S = e^{-i\theta_S} S', \tag{3.3}$$

$$\Phi_a = e^{-i\xi_a} \Phi'_a. \tag{3.4}$$

Then, the scalar potential terms take the same forms as the ones given in Eqs. (2.1), (2.4), and (2.5), with the complex parameters being redefined by

$$\mu = e^{i(\theta_2 - \theta_1 + \theta_S)} \mu', \tag{3.5}$$

$$\rho = e^{i(3\theta_S - \xi_3)} \rho', \tag{3.6}$$

$$\mu_\Phi = e^{i(\xi_1 + \xi_2 - \xi_3)} \mu'_\Phi, \tag{3.7}$$

$$c_1 = e^{2i(\theta_2 - \theta_1 + \theta_S)} c'_1, \tag{3.8}$$

$$c_2 = e^{i(-\theta_S + \xi_3 + 2(\theta_2 - \theta_1))} c'_2, \tag{3.9}$$

$$d_1 = e^{i(3\theta_S + \xi_1 + \xi_2)} d'_1, \tag{3.10}$$

$$d_2 = e^{i(\xi_1 + \xi_2 - \xi_3)} d'_2. \tag{3.11}$$

We note that the real parameters in the potential are unchanged under the phase rotations, so we have changed the notations from primed to unprimed, e.g. from  $\mu'$  to  $\mu$ , etc. Then, from the tadpole conditions given in Appendix A, there are two independent CP phases in this model:  $\mu$  and  $\mu_\Phi$  in the renormalizable terms, whose CP phases are supported by those of the dimension-6 operators,  $c_1$  and  $d_2$ , respectively.

In comparison, for two Higgs doublets without  $U(1)'$ , there are extra CP phases from extra quartic couplings for two Higgs doublets, which would give rise to a nontrivial CP phase of the  $\mu$  term by the tadpole conditions [13].

For simplicity, in the following discussion, we focus only on  $(SH_1^\dagger H_2)^2$  among the higher dimensional operators in our model, while the other higher-dimensional terms are set to

zero. In this case, the nonzero CP phases come from  $\mu = \mu_R + i\mu_I$  and  $c_1 = c_R + ic_I$ . Then, in the basis where the CP phases of the VEVs are absorbed into the complex parameters according to Eqs. (3.2)–(3.4), we obtain the squared mass matrix for neutral scalar fields with  $(\rho_1, \rho_2, S_R, \eta_1, \eta_2, S_I)$ , given by

$$M^2 = \begin{pmatrix} M_S^2 & M_{\text{mix}}^2 \\ (M_{\text{mix}}^2)^T & M_P^2 \end{pmatrix} \quad (3.12)$$

where the mass matrices for CP-even, CP-odd scalars and the mixing mass matrix are

$$M_S^2 = \begin{pmatrix} 2\lambda_1 v_1^2 + \frac{\mu_R v_2 v_s}{\sqrt{2}v_1} & 2v_1 v_2 (\lambda_3 + \lambda_4) - \frac{\mu_R v_s}{\sqrt{2}} + \frac{c_R}{\Lambda^2} v_1 v_2 v_s^2 & 2\kappa_1 v_1 v_s - \frac{\mu_R v_2}{\sqrt{2}} + \frac{c_R}{\Lambda^2} v_1 v_2^2 v_s \\ 2v_1 v_2 (\lambda_3 + \lambda_4) - \frac{\mu_R v_s}{\sqrt{2}} + \frac{c_R}{\Lambda^2} v_1 v_2^2 v_s & 2\lambda_2 v_2^2 + \frac{\mu_R v_1 v_s}{\sqrt{2}v_2} & 2\kappa_2 v_2 v_s - \frac{\mu_R v_1}{\sqrt{2}} + \frac{c_R}{\Lambda^2} v_1^2 v_2 v_s \\ 2\kappa_1 v_1 v_s - \frac{\mu_R v_2}{\sqrt{2}} + \frac{c_R}{\Lambda^2} v_1 v_2^2 v_s & 2\kappa_2 v_2 v_s - \frac{\mu_R v_1}{\sqrt{2}} + \frac{c_R}{\Lambda^2} v_1^2 v_2 v_s & 2\lambda_S v_s^2 + \frac{\mu_R v_1 v_2}{\sqrt{2}v_s} \end{pmatrix}, \quad (3.13)$$

$$M_P^2 = \begin{pmatrix} \frac{\mu_R v_2 v_s}{\sqrt{2}v_1} - \frac{c_R}{\Lambda^2} v_2^2 v_s^2 & -\frac{1}{\sqrt{2}}\mu_R v_s + \frac{c_R}{\Lambda^2} v_1 v_2 v_s^2 & -\frac{1}{\sqrt{2}}\mu_R v_2 + \frac{c_R}{\Lambda^2} v_1 v_2^2 v_s \\ -\frac{1}{\sqrt{2}}\mu_R v_s + \frac{c_R}{\Lambda^2} v_1 v_2 v_s^2 & \frac{\mu_R v_1 v_s}{\sqrt{2}v_2} - \frac{c_R}{\Lambda^2} v_1^2 v_s^2 & \frac{1}{\sqrt{2}}\mu_R v_1 - \frac{c_R}{\Lambda^2} v_1^2 v_2 v_s \\ -\frac{1}{\sqrt{2}}\mu_R v_2 + \frac{c_R}{\Lambda^2} v_1 v_2^2 v_s & \frac{1}{\sqrt{2}}\mu_R v_1 - \frac{c_R}{\Lambda^2} v_1^2 v_2 v_s & \frac{\mu_R v_1 v_2}{\sqrt{2}v_s} - \frac{c_R}{\Lambda^2} v_1^2 v_2^2 \end{pmatrix}, \quad (3.14)$$

and

$$M_{\text{mix}}^2 = \frac{1}{\sqrt{2}}\mu_I \begin{pmatrix} \frac{v_2 v_s}{v_1} & -v_s & -v_2 \\ v_s & -\frac{v_1 v_s}{v_2} & -v_1 \\ v_2 & -v_1 & -\frac{v_1 v_2}{v_s} \end{pmatrix}. \quad (3.15)$$

Here, we have used the tadpole condition, which gives rise to the relation between the CP-violating mass term and the coefficient of the dimension-6 operator,

$$\frac{c_I}{\Lambda^2} = \frac{\sqrt{2}\mu_I}{v_1 v_2 v_s}. \quad (3.16)$$

Working in the basis of  $(\rho_1, \rho_2, S_R, A^0)$ , where  $A^0$  is the CP-odd Higgs in the absence of CP violation, and following the details in Appendix B, the squared mass matrix is given in

the following  $4 \times 4$  matrix form,  $M_0^2$ , with

$$\begin{aligned}
(M_0^2)_{11} &= 2\lambda_1 v_1^2 + \frac{\mu_R v_2 v_s}{\sqrt{2} v_1}, \\
(M_0^2)_{12} &= (M_0^2)_{21} = 2v_1 v_2 (\lambda_3 + \lambda_4) - \frac{\mu_R v_s}{\sqrt{2}} + \frac{c_R}{\Lambda^2} v_1 v_2 v_s^2, \\
(M_0^2)_{13} &= (M_0^2)_{31} = 2\kappa_1 v_1 v_s - \frac{\mu_R v_2}{\sqrt{2}} + \frac{c_R}{\Lambda^2} v_1 v_2^2 v_s, \\
(M_0^2)_{14} &= (M_0^2)_{41} = \frac{\mu_I v v_s}{\sqrt{2} v_1} N_A^{-1}, \\
(M_0^2)_{22} &= 2\lambda_2 v_2^2 + \frac{\mu_R v_1 v_s}{\sqrt{2} v_2}, \\
(M_0^2)_{23} &= (M_0^2)_{32} = 2\kappa_2 v_2 v_s - \frac{\mu_R v_1}{\sqrt{2}} + \frac{c_R}{\Lambda^2} v_1^2 v_2 v_s, \\
(M_0^2)_{24} &= (M_0^2)_{42} = \frac{\mu_I v v_s}{\sqrt{2} v_2} N_A^{-1}, \\
(M_0^2)_{33} &= 2\lambda_S v_s^2 + \frac{\mu_R v_1 v_2}{\sqrt{2} v_s}, \\
(M_0^2)_{34} &= (M_0^2)_{43} = \frac{\mu_I v}{\sqrt{2}} N_A^{-1}, \\
(M_0^2)_{44} &= \frac{v^2 v_s}{\sqrt{2} v_1 v_2} \left( \mu_R - \frac{\sqrt{2} c_R v_1 v_2 v_s}{\Lambda^2} \right) N_A^{-2}.
\end{aligned} \tag{3.17}$$

Therefore, the imaginary part of the  $\mu$  parameter,  $\mu_I$ , mixes the CP-even scalars and the CP-odd scalar. We note that the original basis is related to the new basis by

$$\begin{pmatrix} \rho_1 \\ \rho_2 \\ S_R \\ \eta_1 \\ \eta_2 \\ S_I \end{pmatrix} = \mathcal{R} \begin{pmatrix} \rho_1 \\ \rho_2 \\ S_R \\ A^0 \\ G_Y \\ G' \end{pmatrix} \tag{3.18}$$

with

$$\mathcal{R} = \begin{pmatrix} 1_{3 \times 3} & 0 \\ 0 & \mathcal{R}_3 \end{pmatrix}, \tag{3.19}$$

where  $\mathcal{R}_3$  is the  $3 \times 3$  transformation matrix, given in Eq. (B.5). We still need to diagonalize the above  $4 \times 4$  matrix in Eq. (3.17).

### 3.2 Mixing between CP-even and odd scalars

Using the results in the previous subsection and choosing a new basis diagonalizing the  $3 \times 3$  sub-matrix for CP-even scalars in Appendix B, the  $4 \times 4$  matrix in Eq. (3.17) becomes

$$R_h M_{4 \times 4}^2 R_h^T = \begin{pmatrix} R_h M_{3 \times 3}^2 R_h^T & R_h E \\ E^T R_h^T & m_{h_4}^2 \end{pmatrix} \tag{3.20}$$



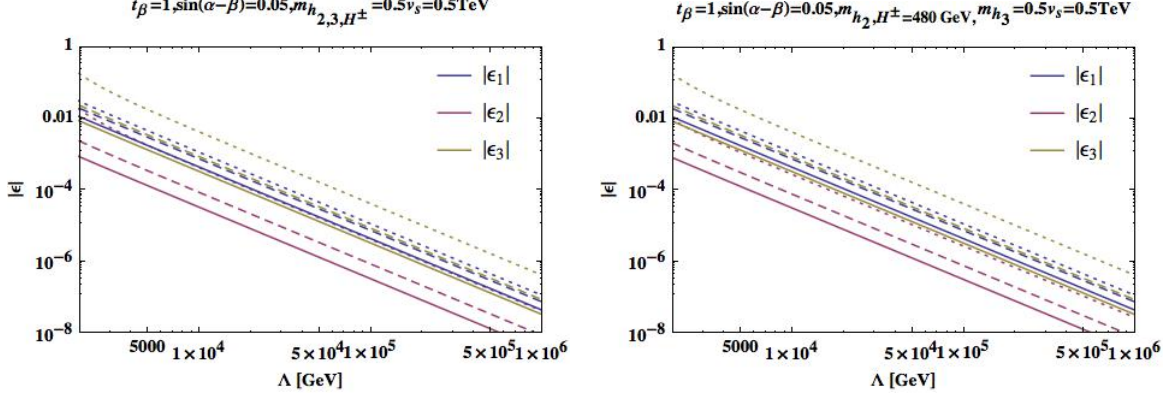


Figure 1: The CP-violating mixing parameters,  $\varepsilon_i$  ( $i = 1, 2, 3$ ), as a function of the cutoff scale for degenerate and non-degenerate case, see Fig. 3 for eEDM predictions. The dotted, dashed, and solid lines represent the case for  $\mu_R = 200, 300,$  and  $500$  GeV respectively. We have taken  $\tan \beta = 1$ ,  $\sin(\alpha - \beta) = 0.05$ , and  $v_s = 1$  TeV.

with

$$E = \frac{\mu_I v_s}{\sqrt{2}} N_A^{-1} \begin{pmatrix} \frac{v}{v_1} \\ \frac{v}{v_2} \\ \frac{v}{v_s} \end{pmatrix}, \quad N_A = \frac{1}{\sqrt{1 + \frac{v_1^2 v_2^2}{v^2 v_s^2}}}. \quad (3.21)$$

Therefore, treating the off-diagonal entries as perturbations, we obtain the approximate mass eigenvalues and mass eigenstates as follows.

$$m_{h_n}^2 = m_{h_n^0}^2 + \Delta_{nn} + \sum_{k \neq n} \frac{|\Delta_{nk}|^2}{m_{h_n^0}^2 - m_{h_k^0}^2} + \dots, \quad (3.22)$$

where  $m_{h_n}^2$  are the mass eigenvalues for zero off-diagonal components containing the fourth row or column [11] up to the corrections from the dimension-6 operator, given in Eqs. (B.11) and (B.13) in Appendix B, and

$$h_n = h_n^0 + \sum_{k \neq n} \frac{\Delta_{kn}}{m_{h_n^0}^2 - m_{h_k^0}^2} h_k^0 + \dots \quad (3.23)$$

with

$$\Delta = \begin{pmatrix} 0 & R_h E \\ E^T R_h^T & 0 \end{pmatrix}. \quad (3.24)$$

When the Higgs mixings with the CP-even singlet scalar are small, the rotation matrix between CP-even scalars is approximated as\*

$$R_h \simeq \begin{pmatrix} \cos \alpha & \sin \alpha & 0 \\ -\sin \alpha & \cos \alpha & 0 \\ 0 & 0 & 1 \end{pmatrix} \quad (3.25)$$

\*We note that our conventions for the Higgs mixing are different from those in the main text of our previous work [11].

with  $\alpha = \alpha_1$  and  $\alpha_2 \simeq \alpha_3 \simeq 0$ . In this case, we can further simplify the above results as

$$m_{h_1}^2 \approx m_{h_1^0}^2 + \varepsilon_1 (R_h E)_1, \quad (3.26)$$

$$m_{h_2}^2 \approx m_{h_2^0}^2 + \varepsilon_2 (R_h E)_2, \quad (3.27)$$

$$m_{h_3}^2 \approx m_{h_3^0}^2 + \varepsilon_3 (R_h E)_3, \quad (3.28)$$

$$m_{h_4}^2 \approx m_{h_4^0}^2 - \varepsilon_1 (R_h E)_1 - \varepsilon_2 (R_h E)_2 - \varepsilon_3 (R_h E)_3, \quad (3.29)$$

and

$$h_1 \approx \cos \alpha \rho_1 + \sin \alpha \rho_2 + \varepsilon_1 A^0, \quad (3.30)$$

$$h_2 \approx -\sin \alpha \rho_1 + \cos \alpha \rho_2 + \varepsilon_2 A^0, \quad (3.31)$$

$$h_3 \approx S_R + \varepsilon_3 A^0, \quad (3.32)$$

$$h_4 \approx A^0 + (-c_\alpha \varepsilon_1 + s_\alpha \varepsilon_2) \rho_1 - (s_\alpha \varepsilon_1 + c_\alpha \varepsilon_2) \rho_2 - \varepsilon_3 S_R \quad (3.33)$$

Here, noting that  $\varepsilon_n \equiv (R_h E)_n / (m_{h_n^0}^2 - m_{h_4^0}^2)$ , which results in

$$\varepsilon_1 = \frac{1}{m_{h_1^0}^2 - m_{h_4^0}^2} \frac{\mu_I v_s}{\sqrt{2} N_A} \left( \frac{s_\alpha}{s_\beta} + \frac{c_\alpha}{c_\beta} \right), \quad (3.34)$$

$$\varepsilon_2 = \frac{1}{m_{h_2^0}^2 - m_{h_4^0}^2} \frac{\mu_I v_s}{\sqrt{2} N_A} \left( \frac{c_\alpha}{s_\beta} - \frac{s_\alpha}{c_\beta} \right), \quad (3.35)$$

$$\varepsilon_3 = \frac{1}{m_{h_3^0}^2 - m_{h_4^0}^2} \frac{\mu_I v_s}{\sqrt{2} N_A}, \quad (3.36)$$

we can write the original scalar fields in terms of the approximate mass eigenstates as

$$\rho_1 \approx c_\alpha h_1 - s_\alpha h_2 + (-c_\alpha \varepsilon_1 + s_\alpha \varepsilon_2) h_4, \quad (3.37)$$

$$\rho_2 \approx s_\alpha h_1 + c_\alpha h_2 + (-s_\alpha \varepsilon_1 - c_\alpha \varepsilon_2) h_4, \quad (3.38)$$

$$S_R \approx h_3 - \varepsilon_3 h_4, \quad (3.39)$$

$$A^0 \approx h_4 + \varepsilon_1 h_1 + \varepsilon_2 h_2 + \varepsilon_3 h_3. \quad (3.40)$$

As a consequence, we find from Eqs. (3.34)–(3.36) that close to the alignment limit where  $\alpha = \beta$ , the CP-violating parameters in the Higgs mixing become

$$\varepsilon_1 \simeq -1.2 \times 10^{-3} \left( \frac{625 \text{ GeV}}{m_{h_4^0} + m_{h_1^0}} \right) \left( \frac{375 \text{ GeV}}{m_{h_4^0} - m_{h_1^0}} \right) \left( \frac{v_s}{1 \text{ TeV}} \right) \left( \frac{\mu_I}{0.2 \text{ GeV}} \right), \quad (3.41)$$

$$\varepsilon_2 \simeq -4.4 \times 10^{-3} \left( \frac{950 \text{ GeV}}{m_{h_4^0} + m_{h_2^0}} \right) \left( \frac{50 \text{ GeV}}{m_{h_4^0} - m_{h_2^0}} \right) \left( \frac{v_s}{1 \text{ TeV}} \right) \left( \frac{\mu_I}{0.2 \text{ GeV}} \right), \quad (3.42)$$

$$\varepsilon_3 \simeq -2.9 \times 10^{-3} \left( \frac{950 \text{ GeV}}{m_{h_4^0} + m_{h_3^0}} \right) \left( \frac{50 \text{ GeV}}{m_{h_4^0} - m_{h_3^0}} \right) \left( \frac{v_s}{1 \text{ TeV}} \right) \left( \frac{\mu_I}{0.2 \text{ GeV}} \right). \quad (3.43)$$

Here, the typical value for  $\mu_I$  was taken from Eq. (3.16) for  $\Lambda / \sqrt{|c_I|} \simeq 10 \text{ TeV}$ .

In Fig. 1, we depict the CP-violating mixing parameters,  $|\varepsilon_i|$  ( $i = 1, 2, 3$ ), as a function of the cutoff scale for different  $\mu_R$ . For instance, for  $\tan \beta = 1$  and  $\mu_R = 100 \text{ GeV} - 1 \text{ TeV}$ ,

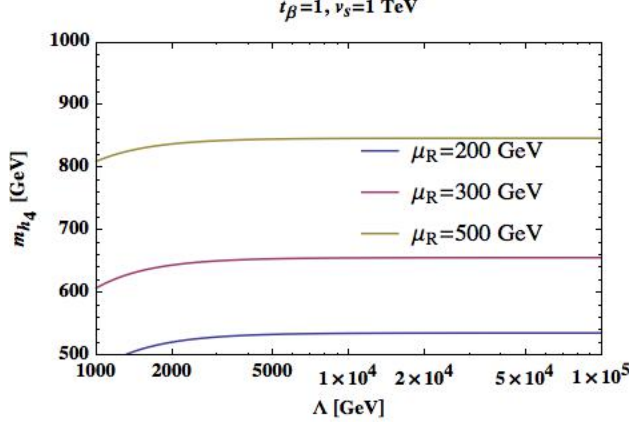


Figure 2: The mass of the pseudoscalar-like Higgs,  $m_{h_4}$ , vs the cutoff scale, for  $\mu_R = 200, 300, 500$  GeV for upper, middle, and lower lines, respectively.

the VEV of the singlet scalar field,  $v_s$ , is bounded as  $250 \text{ GeV} \lesssim v_s \lesssim 2 \text{ TeV}$  [11] in the alignment limit. Thus, in order to choose a larger  $v_s$  for heavy  $Z'$ , a smaller  $\mu_R$  is favored by unitarity. The figure shows that the smaller  $\mu_R$ , the larger the CP-violating mixing predicted, as indicated by Eqs. (3.41), (3.42), and (3.43). Moreover, the larger the mass splitting between  $h_{1,2,3}$  and  $h_4$ , the smaller magnitude  $\varepsilon_i$ .

Since the pseudoscalar-like Higgs mixes with the CP-even scalars due to the CP violation, it is important to identify the allowed mass range of the pseudoscalar-like Higgs in our model. In Fig. 2, we show the range of masses for the pseudoscalar-like Higgs,  $m_{h_4}$ , and the cutoff scale. As a result,  $m_{h_4}$  becomes almost independent of the cutoff scale with  $\Lambda \gtrsim 2 \text{ TeV}$ , so it can be determined mainly by the  $\mu_R$  parameter. Thus, we find that as  $\mu_R$  increase,  $m_{h_4}$  becomes larger, according to Eq. (B.13).

We also remark that the charged Higgs mass is not affected by the CP violation, so it is given in Eq. (B.15) as in Ref. [11] without CP violation.

## 4 Yukawa couplings with CP violation

In this section, we present the mass matrices for the SM fermions and the flavor-changing couplings for quarks in our model. The results provide a complete basis for studying electric dipole moments, collider searches and magnetic dipole moments of leptons in the next section, together with the Higgs mixing in the previous section.

For the phase-rotated scalar fields with Eqs. (3.2)–(3.4), we can rewrite the Yukawa couplings for quarks and leptons as follows.

$$\begin{aligned}
 -\mathcal{L}_Y = & \bar{q}'_i (e^{-i\theta_1} y'_{ij}{}^u \tilde{H}_1 + e^{-i\theta_2} h'_{ij}{}^u \tilde{H}_2) u'_j + \bar{q}'_i (e^{i\theta_1} y'_{ij}{}^d H_1 + e^{i\theta_2} h'_{ij}{}^d H_2) d'_j \\
 & + e^{i\theta_1} y'_{ij}{}^\ell \bar{\ell}'_i H_1 e'_j + e^{-i\theta_1} y'_{ij}{}^\nu \bar{\ell}'_i \tilde{H}_1 \nu'_{jR} + \frac{1}{2} (\nu'_{iR})^c (M_{ij} + e^{i\theta_{\varepsilon_a}} z'_{ij}{}^{(a)} \Phi_a) \nu'_{jR} + \text{h.c.} \quad (4.1)
 \end{aligned}$$

Then, after the scalars get nonzero VEVs, we obtain the quark and lepton mass terms as

$$\mathcal{L}_Y = -\bar{u}'_L M_u u'_R - \bar{d}'_L M_d d'_R - \bar{\ell}'_L M'_\ell \ell'_R - \bar{\ell}'_L M_D \nu'_R - \frac{1}{2} \overline{(\nu'_R)^c} M_R \nu'_R + \text{h.c.} \quad (4.2)$$

with the following flavor structure:

$$M_u = \begin{pmatrix} y_{11}^u \langle \tilde{H}_1 \rangle & y_{12}^u \langle \tilde{H}_1 \rangle & 0 \\ y_{21}^u \langle \tilde{H}_1 \rangle & y_{22}^u \langle \tilde{H}_1 \rangle & 0 \\ h_{31}^u \langle \tilde{H}_2 \rangle & h_{32}^u \langle \tilde{H}_2 \rangle & y_{33}^u \langle \tilde{H}_1 \rangle \end{pmatrix}, \quad (4.3)$$

$$M_d = \begin{pmatrix} y_{11}^d \langle H_1 \rangle & y_{12}^d \langle H_1 \rangle & h_{13}^d \langle H_2 \rangle \\ y_{21}^d \langle H_1 \rangle & y_{22}^d \langle H_1 \rangle & h_{23}^d \langle H_2 \rangle \\ 0 & 0 & y_{33}^d \langle H_1 \rangle \end{pmatrix}, \quad (4.4)$$

$$M_\ell = \begin{pmatrix} y_{11}^\ell \langle H_1 \rangle & 0 & 0 \\ 0 & y_{22}^\ell \langle H_1 \rangle & 0 \\ 0 & 0 & y_{33}^\ell \langle H_1 \rangle \end{pmatrix}, \quad (4.5)$$

$$M_D = \begin{pmatrix} y_{11}^\nu \langle \tilde{H}_1 \rangle & 0 & 0 \\ 0 & y_{22}^\nu \langle \tilde{H}_1 \rangle & 0 \\ 0 & 0 & y_{33}^\nu \langle \tilde{H}_1 \rangle \end{pmatrix}, \quad (4.6)$$

$$M_R = \begin{pmatrix} M_{11} & z_{12}^{(1)} \langle \Phi_1 \rangle & z_{13}^{(2)} \langle \Phi_2 \rangle \\ z_{21}^{(1)} \langle \Phi_1 \rangle & 0 & z_{23}^{(3)} \langle \Phi_3 \rangle \\ z_{31}^{(2)} \langle \Phi_2 \rangle & z_{32}^{(3)} \langle \Phi_3 \rangle & 0 \end{pmatrix}. \quad (4.7)$$

Here, we absorbed the Higgs phases into the Yukawa couplings by  $y_{ij}^u = e^{-i\theta_1} y_{ij}^{\prime u}$ ,  $h_{ij}^u = e^{-i\theta_2} h_{ij}^{\prime u}$ , etc. Since the mass matrix for charged leptons is already diagonal, the lepton mixings come from the mass matrix of right-handed neutrinos. There are four categories of neutrino mixing matrices, that are compatible with neutrino data for at least three complex scalar fields with different  $U(1)'$  charges [11].

## 4.1 Quark mass matrices

After two Higgs doublet fields develop VEVs, we obtain the quark mass matrices from Eqs. (4.3) and (4.4) as

$$(M_u)_{ij} = \frac{1}{\sqrt{2}} v \cos \beta \begin{pmatrix} y_{11}^u & y_{12}^u & 0 \\ y_{21}^u & y_{22}^u & 0 \\ 0 & 0 & y_{33}^u \end{pmatrix} + \frac{1}{\sqrt{2}} v \sin \beta \begin{pmatrix} 0 & 0 & 0 \\ 0 & 0 & 0 \\ h_{31}^u & h_{32}^u & 0 \end{pmatrix},$$

$$(M_d)_{ij} = \frac{1}{\sqrt{2}} v \cos \beta \begin{pmatrix} y_{11}^d & y_{12}^d & 0 \\ y_{21}^d & y_{22}^d & 0 \\ 0 & 0 & y_{33}^d \end{pmatrix} + \frac{1}{\sqrt{2}} v \sin \beta \begin{pmatrix} 0 & 0 & h_{13}^d \\ 0 & 0 & h_{23}^d \\ 0 & 0 & 0 \end{pmatrix}. \quad (4.8)$$

The above quark mass matrices can be diagonalized by

$$U_L^\dagger M_u U_R = M_u^D = \begin{pmatrix} m_u & 0 & 0 \\ 0 & m_c & 0 \\ 0 & 0 & m_t \end{pmatrix}, \quad D_L^\dagger M_d D_R = M_d^D = \begin{pmatrix} m_d & 0 & 0 \\ 0 & m_s & 0 \\ 0 & 0 & m_b \end{pmatrix}, \quad (4.9)$$

thus the CKM matrix is given as  $V_{\text{CKM}} = U_L^\dagger D_L$ . We note that the Yukawa couplings of the second Higgs doublet are sources of flavor violation, which could be important in meson decays/mixings and collider searches for flavor-violating top decays and/or heavy Higgs bosons.

Since  $h_{31}^u$  and  $h_{32}^u$  correspond to rotations of right-handed up-type quarks, we can take  $U_L = 1$ , so  $V_{\text{CKM}} = D_L$ . In this case, we have an approximate relation for the down-type quark mass matrix,  $M_d \approx V_{\text{CKM}} M_d^D$ , up to  $m_{d,s}/m_b$  corrections. Then the Yukawa couplings between the third and first two generations are given as follows.

$$h_{13}^d = \frac{\sqrt{2}m_b}{v \sin \beta} V_{ub}, \quad h_{23}^d = \frac{\sqrt{2}m_b}{v \sin \beta} V_{cb}. \quad (4.10)$$

For  $V_{ub} \simeq 0.004 \ll V_{cb} \simeq 0.04$ , we have  $h_{13}^d \ll h_{23}^d$ . The down-type Yukawa couplings are determined as

$$\begin{aligned} y_{11}^d &= \frac{\sqrt{2}m_d}{v \cos \beta} V_{ud}, & y_{12}^d &= \frac{\sqrt{2}m_s}{v \cos \beta} V_{us}, \\ y_{21}^d &= \frac{\sqrt{2}m_d}{v \cos \beta} V_{cd}, & y_{22}^d &= \frac{\sqrt{2}m_s}{v \cos \beta} V_{cs}, & y_{33}^d &= \frac{\sqrt{2}m_b}{v \cos \beta} V_{tb}. \end{aligned} \quad (4.11)$$

Therefore, we have fixed the down-type Yukawa couplings completely, including the weak CP phase.

Furthermore, taking  $U_L = 1$  as above, we find another approximate relation for the up-type quark mass matrix:  $M_u = M_u^D U_R^\dagger$ . Then, the rotation mass matrix for right-handed down-type quarks becomes  $U_R^\dagger = (M_u^D)^{-1} M_u$ , which is given as

$$U_R^\dagger = \frac{1}{\sqrt{2}} \begin{pmatrix} \frac{v}{m_u} \cos \beta y_{11}^u & \frac{v}{m_u} \cos \beta y_{12}^u & 0 \\ \frac{v}{m_c} \cos \beta y_{21}^u & \frac{v}{m_c} \cos \beta y_{22}^u & 0 \\ \frac{v}{m_t} \sin \beta h_{31}^u & \frac{v}{m_t} \sin \beta h_{32}^u & \frac{v}{m_t} \cos \beta y_{33}^u \end{pmatrix}. \quad (4.12)$$

From the unitarity condition of  $U_R$  we further find the following constraints on the up-type quark Yukawa couplings:

$$|y_{11}^u|^2 + |y_{12}^u|^2 = \frac{2m_u^2}{v^2 \cos^2 \beta}, \quad (4.13)$$

$$|y_{21}^u|^2 + |y_{22}^u|^2 = \frac{2m_c^2}{v^2 \cos^2 \beta}, \quad (4.14)$$

$$|y_{33}^u|^2 + \tan^2 \beta (|h_{31}^u|^2 + |h_{32}^u|^2) = \frac{2m_t^2}{v^2 \cos^2 \beta}, \quad (4.15)$$

$$y_{11}^u (y_{21}^u)^* + y_{12}^u (y_{22}^u)^* = 0, \quad (4.16)$$

$$y_{21}^u (h_{31}^u)^* + y_{22}^u (h_{32}^u)^* = 0, \quad (4.17)$$

$$y_{11}^u (h_{31}^u)^* + y_{12}^u (h_{32}^u)^* = 0. \quad (4.18)$$

Now we are in a position to show the absence of the extra CP phases in the quark Yukawa couplings in our model. First, performing the simultaneous phase rotations of  $q_L$

and  $u_R$  as well as  $d_R$  to leave the down-type Yukawa couplings untouched, we can eliminate the CP phases in the diagonal entries,  $y_{ii}^u$  with  $i = 1, 2, 3$ . Then, there are four CP phases from  $y_{12}^u, y_{21}^u, h_{31}^u, h_{32}^u$ , subject to three unitarity conditions in Eqs. (4.16)–(4.18). Therefore, there remains only one independent CP phase, other than the weak CP phase in the SM. Suppose that off-diagonal entries in the up-type Yukawa matrix are nonzero, so we write  $y_{21}^u = e^{i\theta_{21}}|y_{21}^u|$ ,  $y_{12}^u = e^{i\theta_{12}}|y_{12}^u|$ ,  $h_{31}^u = e^{i\theta_{31}}|h_{31}^u|$  and  $h_{32}^u = e^{i\theta_{32}}|h_{32}^u|$ . Then, Eqs. (4.16)–(4.18) lead to

$$e^{i(\theta_{21}+\theta_{12})} = -\frac{|y_{11}^u y_{21}^u|}{|y_{22}^u y_{12}^u|}, \quad (4.19)$$

$$e^{i(\theta_{31}-\theta_{21}-\theta_{32})} = -\frac{|y_{21}^u h_{31}^u|}{|y_{22}^u h_{32}^u|}, \quad (4.20)$$

$$e^{i(\theta_{31}+\theta_{12}-\theta_{32})} = -\frac{|y_{11}^u h_{31}^u|}{|y_{12}^u h_{32}^u|}. \quad (4.21)$$

But, dividing Eq. (4.21) by (4.20), we find that  $e^{i(\theta_{21}+\theta_{12})} = |y_{11}^u y_{22}^u|/|y_{12}^u y_{21}^u|$ . Then, we would get  $|y_{22}^u|^2 + |y_{21}^u|^2 = 0$  with Eq. (4.19), which is inconsistent with Eq. (4.14). Therefore, we must choose  $y_{21}^u = y_{12}^u = h_{31}^u = h_{32}^u = 0$ , for which Eqs. (4.16)–(4.18) are trivially satisfied. As a result, we find that there is no extra CP phase in the up-type Yukawa couplings either. Taking  $y_{21}^u = y_{12}^u = h_{31}^u = h_{32}^u = 0$ , Eqs. (4.13)–(4.15) determine the diagonal down-type Yukawa couplings as

$$|y_{11}^u| = \frac{\sqrt{2}m_u}{v \cos \beta}, \quad |y_{22}^u| = \frac{\sqrt{2}m_c}{v \cos \beta}, \quad |y_{33}^u| = \frac{\sqrt{2}m_t}{v \cos \beta}. \quad (4.22)$$

## 4.2 Quark Yukawa couplings

We begin with the quark Yukawa couplings to the neutral scalars in the interaction basis,

$$\begin{aligned} -\mathcal{L}_Y^h &= \bar{d}_L \left[ \frac{1}{v_1} M_d^D (\rho_1 + i\eta_1) + \frac{1}{\sqrt{2}} \left( -\frac{v_2}{v_1} (\rho_1 + i\eta_1) + (\rho_2 + i\eta_2) \right) \tilde{h}^d \right] d_R \\ &+ \bar{u}_L \left[ \frac{1}{v_1} M_u^D (\rho_1 - i\eta_1) + \frac{1}{\sqrt{2}} \left( -\frac{v_2}{v_1} (\rho_1 - i\eta_1) + (\rho_2 - i\eta_2) \right) \tilde{h}^u \right] u_R + \text{h.c.} \end{aligned} \quad (4.23)$$

Then, using the Higgs mixing Eqs. (3.37)–(3.40) in the previous section and Eqs. (B.6)–(B.8), the Yukawa terms for the third-generation quarks are now written as

$$\begin{aligned} -\mathcal{L}_Y^h &\supset \frac{1}{\sqrt{2}} \sum_{i=1}^4 \left[ \left( \lambda_t^{h_i} + i\tilde{\lambda}_t^{h_i} \right) \bar{t}_L t_R h_i + \left( \lambda_b^{h_i} + i\tilde{\lambda}_b^{h_i} \right) \bar{b}_L b_R h_i \right] \\ &- \frac{s_{\beta-\alpha}}{\sqrt{2}c_\beta} \bar{b}_L (\tilde{h}_{13}^d d_R + \tilde{h}_{23}^d s_R) h_1 + \frac{c_{\beta-\alpha}}{\sqrt{2}c_\beta} \bar{b}_L (\tilde{h}_{13}^d d_R + \tilde{h}_{23}^d s_R) h_2 \\ &- \frac{iN_A}{\sqrt{2}c_\beta} \bar{b}_L (\tilde{h}_{13}^d d_R + \tilde{h}_{23}^d s_R) (\varepsilon_1 h_1 + \varepsilon_2 h_2 + \varepsilon_3 h_3 + h_4) + \text{h.c.}, \end{aligned} \quad (4.24)$$

where

$$\begin{aligned}
\lambda_t^{h_1} &= \frac{\sqrt{2}m_t c_\alpha}{v c_\beta}, & \lambda_t^{h_2} &= -\frac{\sqrt{2}m_t s_\alpha}{v c_\beta}, & \lambda_t^{h_3} &= 0, & \lambda_t^{h_4} &= \frac{\sqrt{2}(-c_\alpha \varepsilon_1 + s_\alpha \varepsilon_2)m_t}{v c_\beta} \\
\lambda_b^{h_1} &= \frac{\sqrt{2}m_b c_\alpha}{v c_\beta} - \frac{\tilde{h}_{33}^d s_{\beta-\alpha}}{c_\beta}, & \lambda_b^{h_2} &= -\frac{\sqrt{2}m_b s_\alpha}{v c_\beta} + \frac{\tilde{h}_{33}^d c_{\beta-\alpha}}{c_\beta}, & \lambda_b^{h_3} &= 0, \\
\lambda_b^{h_4} &= \frac{\sqrt{2}(-c_\alpha \varepsilon_1 + s_\alpha \varepsilon_2)m_b}{v c_\beta} + \frac{\tilde{h}_{33}^d (s_{\beta-\alpha} \varepsilon_1 - c_{\beta-\alpha} \varepsilon_2)}{c_\beta}, \\
\tilde{\lambda}_t^{h_i} &= -N_A \varepsilon_i \frac{\sqrt{2}m_t t_\beta}{v} \quad (i = 1, 2, 3), & \tilde{\lambda}_t^{h_4} &= -N_A \frac{\sqrt{2}m_t t_\beta}{v}, \\
\tilde{\lambda}_b^{h_i} &= N_A \varepsilon_i \left( \frac{\sqrt{2}m_b t_\beta}{v} - \frac{\tilde{h}_{33}^d}{c_\beta} \right) \quad (i = 1, 2, 3), & \tilde{\lambda}_b^{h_4} &= N_A \left( \frac{\sqrt{2}m_b t_\beta}{v} - \frac{\tilde{h}_{33}^d}{c_\beta} \right). \quad (4.25)
\end{aligned}$$

Here,  $\tilde{h}^d \equiv D_L^\dagger h^d D_R$  and  $\tilde{h}^u \equiv U_L^\dagger h^u U_R$ . Thus, by taking  $U_L = 1$  we get  $\tilde{h}^u = h^u U_R$  and  $\tilde{h}^d = V_{\text{CKM}}^\dagger h^d$ . We note that  $\lambda_t^{h_3}$  and  $\lambda_b^{h_3}$  are vanishing because we have neglected the mixing.

As compared to type-I 2HDM, extra Yukawa couplings in our model are given by

$$\tilde{h}_{13}^d = 1.80 \times 10^{-2} \left( \frac{m_b}{v \sin \beta} \right), \quad (4.26)$$

$$\tilde{h}_{23}^d = 5.77 \times 10^{-2} \left( \frac{m_b}{v \sin \beta} \right), \quad (4.27)$$

$$\tilde{h}_{33}^d = 2.41 \times 10^{-3} \left( \frac{m_b}{v \sin \beta} \right). \quad (4.28)$$

We find that there is no modification in the top quark Yukawa coupling as compared to the SM, whereas down-type quarks can have large flavor-violating couplings if  $\tan \beta$  is small. In the alignment limit where  $\alpha = \beta$ , the flavor-violating interactions of the SM-like Higgs  $h_1$  boson are turned off. In Refs. [10, 11], we have discussed the phenomenological bounds on the sizable flavor-changing couplings for down-type quarks, for instance, the bounds from  $B$ -meson decays ( $B_s \rightarrow \mu^+ \mu^-$ ,  $B_s \rightarrow X \gamma$ ) and mixings ( $B_s - \bar{B}_s$ ), etc, constrain the parameter space for heavy Higgs scalar and  $Z'$  masses.

Moreover, from the resulting Yukawa couplings in Eq. (4.24), the simultaneous presence of scalar and pseudoscalar couplings violate the CP symmetry. In particular, the CP-violating top Yukawa couplings are constrained by the bounds from neutron and electron EDMs. Note that in the alignment limit where  $\alpha = \beta$  and  $\varepsilon_i \ll 1$  *i.e.*,  $\mu_I, m_{h_1}, m_{h_2}, m_{h_3} \ll m_{h_4}$ , the CP violation arises mainly through  $h_2$  and  $h_4$ . There are usual flavor-diagonal Yukawa couplings of neutral scalars to light quarks, including the CP-violating mixing, but they are sub-dominant for the EDM contributions.

The Yukawa terms of the charged Higgs boson are given as

$$- \mathcal{L}_Y^{H^-} = \bar{b}(\lambda_{t_L}^{H^-} P_L + \lambda_{t_R}^{H^-} P_R) t H^- + \bar{b}(\lambda_{c_L}^{H^-} P_L + \lambda_{c_R}^{H^-} P_R) c H^- + \lambda_{u_L}^{H^-} \bar{b} P_L u H^- + \text{h.c.}, \quad (4.29)$$

where

$$\begin{aligned}
\lambda_{t_L}^{H^-} &= \frac{\sqrt{2}m_b \tan \beta}{v} V_{tb}^* - \frac{(V_{\text{CKM}} \tilde{h}^d)_{33}^*}{\cos \beta}, \\
\lambda_{t_R}^{H^-} &= -\frac{\sqrt{2}m_t \tan \beta}{v} V_{tb}^*, \\
\lambda_{c_L}^{H^-} &= \frac{\sqrt{2}m_b \tan \beta}{v} V_{cb}^* - \frac{(V_{\text{CKM}} \tilde{h}^d)_{23}^*}{\cos \beta}, \\
\lambda_{c_R}^{H^-} &= -\frac{\sqrt{2}m_c \tan \beta}{v} V_{cb}^*, \\
\lambda_{u_L}^{H^-} &= \frac{\sqrt{2}m_b \tan \beta}{v} V_{ub}^* - \frac{(V_{\text{CKM}} \tilde{h}^d)_{13}^*}{\cos \beta}
\end{aligned} \tag{4.30}$$

with

$$V_{\text{CKM}} \tilde{h}^d = \begin{pmatrix} 0 & 0 & V_{ud} \tilde{h}_{13}^d + V_{us} \tilde{h}_{23}^d + V_{ub} \tilde{h}_{33}^d \\ 0 & 0 & V_{cd} \tilde{h}_{13}^d + V_{cs} \tilde{h}_{23}^d + V_{cb} \tilde{h}_{33}^d \\ 0 & 0 & V_{td} \tilde{h}_{13}^d + V_{ts} \tilde{h}_{23}^d + V_{tb} \tilde{h}_{33}^d \end{pmatrix}. \tag{4.31}$$

### 4.3 Lepton Yukawa couplings

As can be seen in (4.5), the mass matrix for charged leptons  $e_j$  is already diagonal due to the  $U(1)'$  symmetry. Thus, the lepton Yukawa couplings are in a flavor-diagonal form, given by

$$\begin{aligned}
-\mathcal{L}_Y^\ell &= \frac{m_{e_j} \cos \alpha}{v \cos \beta} \bar{e}_j e_j h_1 - \frac{m_{e_j} \sin \alpha}{v \cos \beta} \bar{e}_j e_j h_2 + \frac{m_{e_j}}{v \cos \beta} \bar{e}_j e_j (-c_\alpha \varepsilon_1 + s_\alpha \varepsilon_2) h_4 \\
&+ \frac{im_{e_j} N_A \tan \beta}{v} \bar{e}_j \gamma^5 e_j (h_4 + \varepsilon_1 h_1 + \varepsilon_2 h_2 + \varepsilon_3 h_3) \\
&+ \frac{\sqrt{2}m_{e_j} \tan \beta}{v} (\bar{\nu}_j P_R e_j H^+ + \text{h.c.}).
\end{aligned} \tag{4.32}$$

As a result, the CP symmetry is also broken in the lepton Yukawa couplings to the neutral scalars.

## 5 $B$ -meson anomalies, EDM and collider searches

We update the status of  $B$ -meson anomalies in light of the updated data and analysis on  $R_{K^{(*)}}$  ratios and review the parameter space for  $Z'$  mass and couplings for the flavored  $U(1)'$  model. Then, we calculate the electric dipole moment of the electron in the presence of the CP-violating mixings between neutral scalars and constrain the extra Higgs masses and the cutoff scale for higher-dimensional operators. We also briefly discuss the anomalous magnetic moments of leptons in our model.



## 5.1 Update on $B$ -meson anomalies

We first remark that the measurement of  $R_K = \mathcal{B}(B \rightarrow K\mu^+\mu^-)/\mathcal{B}(B \rightarrow Ke^+e^-)$  has been updated by the new analysis with LHCb 2015–2016 data [3], showing the combined value with LHCb 2011–2012 data,

$$R_K = 0.846_{-0.054}^{+0.060}(\text{stat})_{-0.014}^{+0.016}(\text{syst}), \quad (5.1)$$

which deviates from the SM prediction by  $2.5\sigma$ . Thus, the updated global fit for  $B$ -meson decays shows that the purely muonic contribution from new physics to the Wilson coefficients,  $C_9^{\mu,\text{NP}} = -C_{10}^{\mu,\text{NP}}$ , is favored from the data for lepton flavor non-universality [8,9], as compared to  $C_9$  only, but  $C_9^{\mu,\text{NP}} \neq 0$  and  $C_{10}^{\mu,\text{NP}} = 0$  is slightly favored for all the data set [9]. Recently, the analysis of the full Belle data sample led to new results on  $R_K$  in various bin energies, in particular, the new Belle result in the bin of interest,  $1 \text{ GeV}^2 < q^2 < 6 \text{ GeV}^2$ , is consistent with the LHCb result [12].

On the other hand for vector  $B$ -mesons,  $R_{K^*} = \mathcal{B}(B \rightarrow K^*\mu^+\mu^-)/\mathcal{B}(B \rightarrow K^*e^+e^-)$  from LHCb [4] is

$$R_{K^*} = \begin{cases} 0.66_{-0.07}^{+0.11}(\text{stat}) \pm 0.03(\text{syst}), & 0.045 \text{ GeV}^2 < q^2 < 1.1 \text{ GeV}^2, \\ 0.69_{-0.07}^{+0.11}(\text{stat}) \pm 0.05(\text{syst}), & 1.1 \text{ GeV}^2 < q^2 < 6.0 \text{ GeV}^2, \end{cases} \quad (5.2)$$

which again differs from the SM prediction by  $2.1$ – $2.3\sigma$  and  $2.4$ – $2.5\sigma$ , depending on the energy bins. The deviation in  $R_{K^*}$  is supported by the reduction in the angular distribution of  $B \rightarrow K^*\mu^+\mu^-$  [5] and the recent update on  $R_{K^*}$  from the Belle data [6], also shows a similar deviation in particular in low energy bins ( $0.045 \text{ GeV} < q^2 < 1.1 \text{ GeV}$ ).

We also remark that there have been intriguing anomalies in  $R_D = \mathcal{B}(B \rightarrow D\tau\nu)/\mathcal{B}(B \rightarrow D\ell\nu)$  and  $R_{D^*} = \mathcal{B}(B \rightarrow D^*\tau\nu)/\mathcal{B}(B \rightarrow D^*\ell\nu)$  with  $\ell = e, \mu$  for BaBar [14] and Belle [15,16] and  $\ell = \mu$  for LHCb [17], although we do not pursue an explanation for these anomalies in our work. In this case, the deviations between the measurements and the SM predictions for  $R_D$  and  $R_{D^*}$  are  $1.4\sigma$  and  $2.5\sigma$ , respectively, amounting to the combined deviation of  $3.08\sigma$  [18]. However, the recent update on  $R_{D^{(*)}}$  with semi-leptonic tagging from Belle [19] shows an agreement with the SM predictions within  $1.6\sigma$  deviations. We do not pursue an explanation of  $R_{D^{(*)}}$  anomalies in our work, but we comment that the SM can be simply extended with leptoquarks to explain the associated anomalies as well as the anomalous magnetic moment of muon [20].

## 5.2 Bounds from $B$ -meson decays

The relevant  $Z'$  interactions for bottom quarks in the flavored  $U(1)'$  model are given by

$$\mathcal{L}_{Z'} = g_{Z'} Z'_\mu \left( \frac{1}{3} x V_{ts}^* V_{tb} \bar{s} \gamma^\mu P_L b + \text{h.c.} + y \bar{\mu} \gamma^\mu \mu \right). \quad (5.3)$$

Then, after integrating out the  $Z'$  gauge boson, we obtain the effective four-fermion interaction for  $\bar{b} \rightarrow \bar{s}\mu^+\mu^-$  as follows.

$$\mathcal{L}_{\text{eff},\bar{b}\rightarrow\bar{s}\mu^+\mu^-} = -\frac{xyg_{Z'}^2}{3m_{Z'}^2} V_{ts}^* V_{tb} (\bar{s}\gamma^\mu P_L b)(\bar{\mu}\gamma_\mu\mu) + \text{h.c.} \quad (5.4)$$

Consequently, as compared to the effective Hamiltonian with the SM normalization,

$$\Delta\mathcal{H}_{\text{eff},\bar{b}\rightarrow\bar{s}\mu^+\mu^-} = -\frac{4G_F}{\sqrt{2}} V_{ts}^* V_{tb} \frac{\alpha_{\text{em}}}{4\pi} C_9^{\mu,\text{NP}} \mathcal{O}_9^\mu \quad (5.5)$$

with  $\mathcal{O}_9^\mu \equiv (\bar{s}\gamma^\mu P_L b)(\bar{\mu}\gamma_\mu\mu)$  and  $\alpha_{\text{em}}$  being the electromagnetic coupling, the new physics contribution to the Wilson coefficient is identified as

$$C_9^{\mu,\text{NP}} = -\frac{8xy\pi^2\alpha_{Z'}}{3\alpha_{\text{em}}} \left(\frac{v}{m_{Z'}}\right)^2 \quad (5.6)$$

with  $\alpha_{Z'} \equiv g_{Z'}^2/(4\pi)$ , and vanishing contributions to other operators,  $C_{10}^{\mu,\text{NP}} = C_9^{\mu,\text{NP}} = C_{10}'^{\mu,\text{NP}} = 0$ . Choosing  $xy > 0$  for a negative sign of  $C_9^\mu$  for  $B$ -meson anomalies from  $R_{K^{(*)}}$  and requiring the best-fit value,  $C_9^{\mu,\text{NP}} = -0.98$  [9], (while taking  $[-1.15, -0.81]$  and  $[-1.31, -0.64]$  within  $1\sigma$  and  $2\sigma$  errors), to explain the  $B$ -meson anomalies together with the full set of the data [9], we get the condition for  $Z'$  mass and couplings as follows:

$$m_{Z'} = 1.27 \text{ TeV} \times \left(xy \frac{\alpha_{Z'}}{\alpha_{\text{em}}}\right)^{1/2}. \quad (5.7)$$

Therefore,  $m_{Z'} \simeq 1 \text{ TeV}$  for  $xy \simeq 1$  and  $\alpha_{Z'} \simeq \alpha_{\text{em}}$ . For values of  $xy$  less than unity or  $\alpha_{Z'} \lesssim \alpha_{\text{em}}$ ,  $Z'$  can be even lighter.

There are various phenomenological constraints on the  $Z'$  for bottom quarks and leptons, coming from dimuon resonance searches,  $B - \bar{B}$  mixings, other meson decays such as  $B \rightarrow X_s\gamma$ , tau lepton decays and neutrino scattering. Taking them into account, it was shown that the parameter space with  $xg_{Z'} \lesssim 0.05$  for  $yg_{Z'} \simeq 1$  and  $m_{Z'} \lesssim 1 \text{ TeV}$  [10, 11] is consistent for  $B$ -meson anomalies. See also the phenomenological discussion on similar models in Ref. [21].

On the other hand, in the presence of sizable flavor violating couplings between down-type quarks and heavy Higgs bosons in Eqs. (4.26) and (4.27), the  $B$ -meson decays,  $B_s \rightarrow \mu^+\mu^-$ ,  $B - \bar{B}$  mixings,  $B \rightarrow X_s\gamma$ , etc, can strongly constrain the parameter space for heavy Higgs bosons in combination of unitarity and perturbativity. For instance, in the alignment limit and for  $\tan\beta = 1$ , the masses of heavy Higgs bosons must be in the range of  $200 \text{ GeV} \lesssim m_{h_4} \lesssim 700 \text{ GeV}$  and  $200 \text{ GeV} \lesssim m_{h_2} = m_{H^+} \lesssim 600 \text{ GeV}$  [10, 11]. For a smaller value of  $\tan\beta$ , all the  $B$ -meson and theoretical bounds become more stringent, due to larger flavor violating couplings, so the masses of heavy Higgs bosons should be almost degenerate and about 300–400 GeV.

### 5.3 Electric dipole moments

The current strongest limit on the electron EDM (eEDM) comes from ACMEII [22],

$$d_e < 1.1 \times 10^{-29} \text{ e cm.} \quad (5.8)$$

In the presence of the general mixings between CP-even and CP-odd scalars, the couplings of physical scalars  $h_i$  ( $i = 1, 2, 3, 4$ ) to the SM fermions and  $W$  and  $Z$  gauge bosons can be parameterized as

$$\mathcal{L} = \sum_{i=1}^4 \left[ -m_f (c_{f,i} \bar{f} f + \tilde{c}_{f,i} \bar{f} i \gamma_5 f) + a_i (2m_W^2 W_\mu W^\mu + m_Z^2 Z_\mu Z^\mu) \right] \frac{h_i}{v}, \quad (5.9)$$

with the coefficients  $c_{f,i}$ ,  $\tilde{c}_{f,i}$  and  $a_i$  shown in the previous section and Appendix C.

We now discuss the contributions of the general scalar couplings to the electron EDM (eEDM). For light fermions, the dominant contributions to their eEDM come from the two-loop Barr-Zee type diagrams [23]. For the effective operator for the eEDM,

$$\mathcal{L}_{\text{eff,EDM}} = -\frac{i}{2} \delta_e \bar{e} \sigma_{\mu\nu} \gamma_5 e F^{\mu\nu}, \quad (5.10)$$

the Wilson coefficient  $\delta_e$  receive various contributions as listed in the following,

$$\delta_e = (\delta_e)_t^{h\gamma\gamma} + (\delta_e)_t^{hZ\gamma} + (\delta_e)_W^{h\gamma\gamma} + (\delta_e)_W^{hZ\gamma} + (\delta_e)_{H^\pm}^{h\gamma\gamma} + (\delta_e)_{H^\pm}^{hZ\gamma} + (\delta_e)_h^{H^\pm W^\mp \gamma} \quad (5.11)$$

where the contributions from the diagrams with effective  $h_i \gamma \gamma$  and  $h_i Z \gamma$  couplings (from integrating out a top quark loop) are, respectively,

$$(\delta_f)_t^{h\gamma\gamma} = -\frac{N_c Q_f Q_t^2 e^2}{64\pi^4} \sum_{i=1}^4 \left[ f(z_t^i) c_{t,i} \tilde{c}_{f,i} + g(z_t^i) \tilde{c}_{t,i} c_{f,i} \right], \quad (5.12)$$

$$(\delta_f)_t^{hZ\gamma} = -\frac{N_c Q_f g_{Z\bar{f}f}^V g_{Z\bar{t}t}^V}{64\pi^4} \sum_{i=1}^4 \left[ \tilde{f} \left( z_t^i, \frac{m_t^2}{M_Z^2} \right) c_{t,i} \tilde{c}_{f,i} + \tilde{g} \left( z_t^i, \frac{m_t^2}{M_Z^2} \right) \tilde{c}_{t,i} c_{f,i} \right]. \quad (5.13)$$

Here,  $z_X^i \equiv m_X^2/M_i^2$ ,  $g_{Z\bar{f}f}^V$  is the vector-current couplings of  $Z$  boson to the fermions, and the loop integral functions are given by

$$\begin{aligned} f(z) &\equiv \frac{z}{2} \int_0^1 dx \frac{1-2x(1-x)}{x(1-x)-z} \ln \frac{x(1-x)}{z}, \\ g(z) &\equiv \frac{z}{2} \int_0^1 dx \frac{1}{x(1-x)-z} \ln \frac{x(1-x)}{z}, \\ \tilde{f}(x, y) &\equiv \frac{yf(x) - xf(y)}{y-x}, \\ \tilde{g}(x, y) &\equiv \frac{yg(x) - xg(y)}{y-x}. \end{aligned} \quad (5.14)$$

The contributions from the  $W$ -bosons and the Goldstone bosons to the  $h_i \gamma \gamma$  and  $h_i Z \gamma$  operators are gauge-invariant, which have been obtained as follows [24–26].

$$(\delta_f)_W^{h\gamma\gamma} = \frac{Q_f e^2}{256\pi^4} \sum_{i=1}^4 \left[ \left( 6 + \frac{1}{z_W^i} \right) f(z_w^i) + \left( 10 - \frac{1}{z_W^i} \right) g(z_w^i) \right]$$

$$+ \frac{3}{4} \left( g(z_W^i) + h(z_W^i) \right) \Big] a_i \tilde{c}_{f,i} , \quad (5.15)$$

$$\begin{aligned} (\delta_f)_{W}^{hZ\gamma} &= \frac{g_{Z\bar{f}f}^V g_{ZW}^2}{256\pi^4} \sum_{i=1}^4 \left[ \left( 6 - \sec^2 \theta_W + \frac{2 - \sec^2 \theta_W}{2z_w^i} \right) \tilde{f}(z_W^i, c_W^2) \right. \\ &\quad + \left( 10 - 3 \sec^2 \theta_W - \frac{2 - \sec^2 \theta_W}{2z_w^i} \right) \tilde{g}(z_W^i, c_W^2) \\ &\quad \left. + \frac{3}{2} \left( g(z_W^i) + h(z_W^i) \right) \right] a_i \tilde{c}_{f,i} \end{aligned} \quad (5.16)$$

where the gauge coupling  $g_{WWZ} = e/\tan \theta_W$ , and  $h(z)$  is the loop function, given by

$$h(z) \equiv \frac{z}{2} \int_0^1 dx \frac{1}{z - x(1-x)} \left( 1 + \frac{z}{z - x(1-x)} \ln \frac{x(1-x)}{z} \right) . \quad (5.17)$$

The contributions from the charged Higgs bosons running in loops also read

$$(\delta_f)_{H^\pm}^{h\gamma\gamma} = \frac{Q_f e^2}{256\pi^4} \sum_i \left[ f(z_\pm^i) - g(z_\pm^i) \right] \bar{\lambda}_i \tilde{c}_{f,i} , \quad (5.18)$$

$$(\delta_f)_{H^\pm}^{hZ\gamma} = \frac{g_{Z\bar{f}f}^V g_{ZH^+H^-}}{256\pi^4} \left( \frac{v}{M_\pm} \right)^2 \sum_i \left[ \tilde{f} \left( z_\pm^i, \frac{M_\pm^2}{m_Z^2} \right) - \tilde{g} \left( z_\pm^i, \frac{M_\pm^2}{m_Z^2} \right) \right] \bar{\lambda}_i \tilde{c}_{f,i} \quad (5.19)$$

where  $z_\pm^i = M_\pm^2/M_i^2$ ,  $g_{ZH^+H^-} = e(1 - \tan^2 \theta_W)/(2 \tan \theta_W)$ , and  $\bar{\lambda}_i = -\lambda_{i+-}/v$  are the effective trilinear scalar couplings between neutral and charged scalars, which enter the  $h_i\gamma\gamma$  coupling through the  $H^\pm$  loop. Finally, contributions coming from the  $H^\pm W^\mp \gamma$  operators [26] read

$$(\delta_f)_h^{H^\pm W^\mp \gamma} = \frac{s_f}{512\pi^4} \sum_i \left[ \frac{e^2}{2s_W^2} \mathcal{I}_4(M_i^2, M_\pm^2) a_i \tilde{c}_{f,i} - \mathcal{I}_5(M_i^2, M_\pm^2) \bar{\lambda}_i \tilde{c}_{f,i} \right] , \quad (5.20)$$

where  $s_f = +1$  ( $s_f = -1$ ) for the down-type quarks and charged leptons (the up-type quarks), and the two-loop integral functions are

$$\mathcal{I}_{4,5}(M_1^2, M_2^2) \equiv \frac{m_W^2}{M_\pm^2 - m_W^2} [I_{4,5}(m_W, M_1) - I_{4,5}(M_2, M_1)] \quad (5.21)$$

with

$$\begin{aligned} I_4(M_1, M_2) &\equiv \int_0^1 dz (1-z)^2 \left( z - 4 + z \frac{M_\pm^2 - M_2^2}{m_W^2} \right) \\ &\quad \times \frac{M_1^2}{m_W^2(1-z) + M_2^2 z - M_1^2 z(1-z)} \ln \left( \frac{m_W^2(1-z) + M_2^2 z}{M_1^2 z(1-z)} \right) , \end{aligned} \quad (5.22)$$

$$\begin{aligned} I_5(M_1, M_2) &\equiv \int_0^1 dz \frac{M_1^2 z(1-z)^2}{m_W^2(1-z) + M_2^2 z - M_1^2 z(1-z)} \\ &\quad \times \ln \left( \frac{m_W^2(1-z) + M_2^2 z}{M_1^2 z(1-z)} \right) , \end{aligned} \quad (5.23)$$

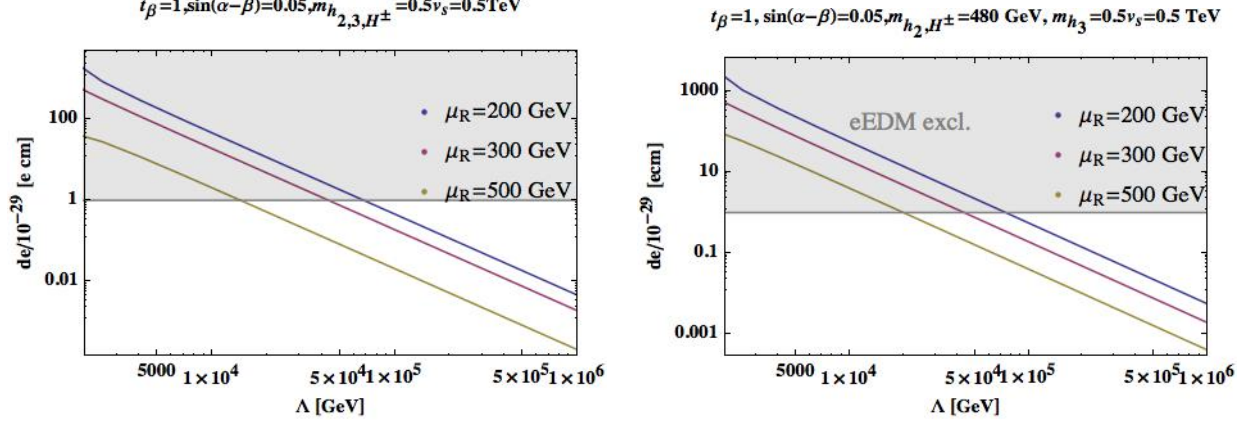


Figure 3: The predicted value of electron EDM as a function of the cutoff scale, for  $\mu_R = 200, 300, 500$  GeV in each plot, respectively. For CP-even like Higgs scalars and charged Higgs, we have taken  $m_{h_2} = m_{h_3} = m_{H^\pm} = 500$  GeV on the left;  $m_{h_2} = m_{H^\pm} = 480$  GeV and  $m_{h_3} = 500$  GeV on the right. We took  $\tan \beta = 1, \sin(\alpha - \beta) = 0.05, v_s = 1$  TeV for both plots. The gray regions are excluded by the limit on the electron EDM comes from ACMEII.

where the relevant trilinear scalar couplings and the couplings among neutral Higgs bosons, charged Higgs bosons and  $W$  bosons are listed in Appendix C.

The eEDM contributions coming from Barr-Zee diagrams involve the neutral scalars,  $h_{1,2,3,4}$ , and the charged Higgs  $H^\pm$ . To demonstrate the relation between the eEDM prediction and the cutoff scale, we consider the alignment scenario with  $\sin(\alpha - \beta) = 0.05$  and  $\tan \beta = 1$ ,  $m_{h_2} = m_{H^\pm}$ , taking into account the electroweak precision bounds as studied in Refs. [10,11]. In Fig. 3, we show the predicted value of electron EDM as a function of the cutoff scale, for degenerate extra scalar masses with  $m_{h_2} = m_{h_3} = m_{H^\pm} = 500$  GeV on the left, and non-degenerate extra scalar masses with  $m_{h_2} = m_{H^\pm} = 480$  GeV and  $m_{h_3} = 500$  GeV on the right panel. The regions shaded in gray have been excluded by the bound on the electron EDM from ACMEII. Here, we find that the larger  $\mu_R$ , the smaller the eEDM value for a fixed cutoff scale, which is consistent with the CP-violating parameters  $\varepsilon_i$  shown in Fig. 1. The degenerate cases confront with a slightly severer bound from ACMEII.

To see the dependence of the eEDM predictions on heavy Higgs masses, in Fig. 4, we show the contours of electron EDM (in units of  $10^{-29}$  e cm) in the parameter space for singlet-like scalar ( $m_{h_3}$ ) and charged Higgs masses ( $m_{H^\pm}$ ). In the case of  $\mu_R = 500$  GeV with cutoff scale  $\Lambda = 20$  TeV, the lowest magnitude of the eEDM is obtained around  $m_{h_3} \simeq 550$  GeV which might be probed by the future eEDM search in ACMEIII, as shown in the left panel. We note that the dominate contribution coming from the  $H^\pm$  loop and  $H^\pm W^\mp \gamma$  cancel to some extent, that is different from the situation studied in Refs. [27–30] where the cancellation mostly occur due to top and  $W$  loops. In the case of  $\mu_R = 300$  GeV, the current ACMEII bound becomes more severe, this it excludes the cutoff scale around  $\Lambda \leq 50$  TeV. Therefore, in this case, we present the prediction of eEDM by choosing a larger value of the cutoff scale,  $\Lambda = 50$  TeV, in the right panel of Fig. 4, so most of the parameter space for heavy Higgs masses is within the sensitivity of the ACMEIII.

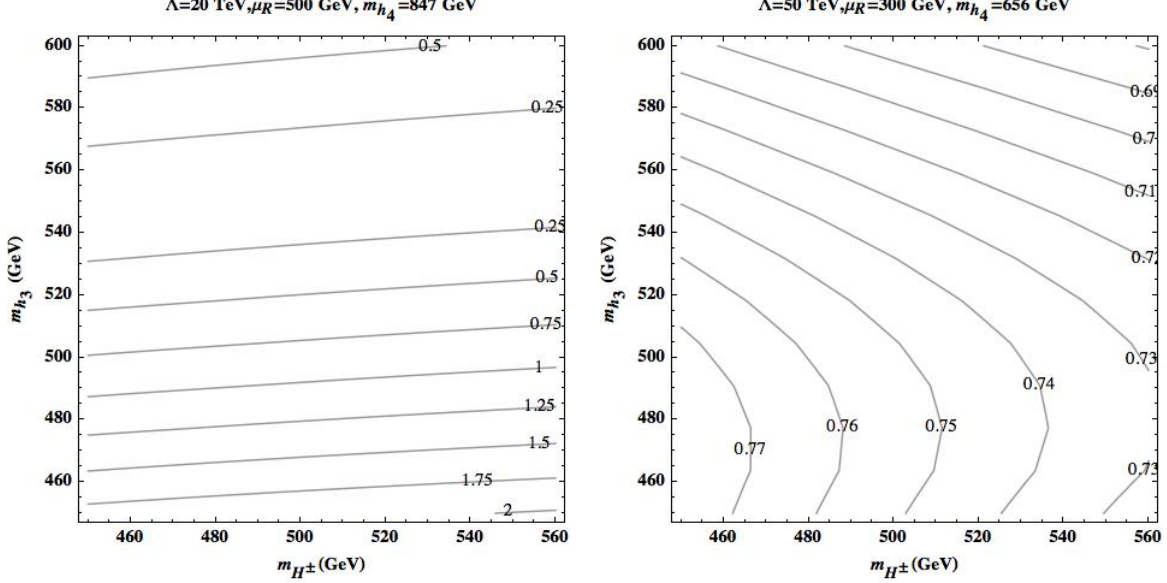


Figure 4: Contours of electron EDM in the parameter space for  $m_{h_3}$  vs  $m_{H^\pm}$ , in units of  $10^{-29}$  e cm.

In summary, the eEDM constraint sets the lower bound on the cutoff scale to be  $\Lambda = 20$ – $50$  TeV, depending on whether the heavy Higgs masses are degenerate or not.

## 5.4 Anomalous magnetic moments of leptons

The measured value for the anomalous magnetic moment of muon has been shown to be deviated from the SM values [31, 32] for quite a while. The recent update on the deviation of the anomalous magnetic moment of muon between experiment and SM values [33] is given by

$$\Delta a_\mu = a_\mu^{\text{exp}} - a_\mu^{\text{SM}} = 279(76) \times 10^{-11}, \quad (5.24)$$

which has  $3.7\sigma$  discrepancy from the SM.

Furthermore, there is a  $2.4\sigma$  discrepancy reported between the SM prediction for the anomalous magnetic moment of electron and the experimental measurements as follows [34, 35]:

$$\Delta a_e = a_e^{\text{exp}} - a_e^{\text{SM}} = -88(36) \times 10^{-14}. \quad (5.25)$$

The magnetic and electric dipole moments of a fermion  $f$  is given by the effective operator,

$$\mathcal{L}_{\text{eff}} = c_{\text{eff}} \bar{f}_L \sigma_{\mu\nu} f_R F^{\mu\nu} + \text{h.c.}, \quad (5.26)$$

for the real and imaginary parts of Wilson coefficient  $c_{\text{eff}}$  [36]. In our model, we consider the two-loop Barr-Zee type diagrams contributions. The muon anomalous dipole moment can

be obtained by changing the couplings as follows.

$$a_\mu = \frac{2m_\mu^2}{eQ_\mu m_e} \times \begin{cases} d_e \begin{pmatrix} c_e \rightarrow \tilde{c}_\mu \\ \tilde{c}_e \rightarrow -c_\mu \end{pmatrix}, & h_i\gamma\gamma, h_i Z\gamma \text{ diagrams} \\ d_e \left( \text{Im}(a_{W^+H^-h_i}) \rightarrow -\text{Re}(a_{W^+H^-h_i}) \right), & W^\pm H_\mp \gamma \text{ diagrams (S)} \\ d_e \left( \text{Im} \left( c_{\tilde{t}_R b_L H^+}^* + c_{\tilde{\nu}_e R H^+} \right) \right. \\ \quad \left. \rightarrow -\text{Re} \left( c_{\tilde{t}_R b_L H^+}^* + c_{\tilde{\nu}_e R H^+} \right) \right), & W^\pm H_\mp \gamma \text{ diagrams (F)} \end{cases}$$

Here, the  $h\gamma\gamma$ ,  $hZ\gamma$  and  $W^\pm H_\mp \gamma$  diagram (S) (with heavy scalars running in the upper loop) contributions to the EDM have been summarized in Refs. [26, 37]. The  $W^\pm H_\mp \gamma$  diagram (F) (with SM fermions running in the upper loop) contributions to the EDM can be found in Refs. [38, 39].

In the parameter space of our interest, consistent with the electroweak precision data and the EDM constraints, we need relatively large masses for heavy Higgs bosons, so the contributions of charged Higgs to the lepton  $g - 2$  are negligible. Thus, we do not pursue the explanation of the deviation in the muon  $g - 2$  in our model.

## 5.5 Collider searches for CP violation

In this subsection, we discuss the independent test of the CP violation from the production of Higgs bosons at the LHC, although the bound from eEDM is already very stringent on the CP-violating mixing between neutral scalars as shown in the previous subsection. The effects of the CP violation arise in the modified Higgs couplings, parameterized by  $\varepsilon_i$ , in comparison with the CP-conserving case. The CP-conserving limit can be attained when  $\varepsilon_i \rightarrow 0$ .

In our study, we have made two assumptions in the Higgs sector. One is that the mixing with the singlet field is negligible, so the singlet-like Higgs boson mostly decouples in the collider phenomenology. We take  $h_3$  to be the singlet-like Higgs boson, while  $h_1$  and  $h_2$  are mostly doublet-like. If the singlet-like Higgs boson is lighter than the others, we can simply relabel the subscript. The other assumption that we have taken is the alignment limit, where  $s_{\alpha-\beta} \rightarrow 0$ , so the non-SM-like Higgs boson  $h_2$  does not couple to the pairs of the electroweak bosons. Still, the couplings of  $h_4$  to  $W^+W^-$  and  $ZZ$  do not vanish, but are proportional to  $\varepsilon_1$ , in the alignment limit:

$$g_{h_4 W^+ W^-} = -\frac{2m_W^2}{v}\varepsilon_1, \quad g_{h_4 Z Z} = -\frac{2m_Z^2}{v}\varepsilon_1. \quad (5.27)$$

However, for  $|\varepsilon_1| \lesssim \mathcal{O}(10^{-3})$  and  $\Lambda > 10$  TeV, the decays of  $h_4$  to the pairs of electroweak bosons would also be suppressed. The dominant decay modes of  $h_4$  are  $h_4 \rightarrow t\bar{t}$  and  $b\bar{b}$  via the  $\tilde{\lambda}_{t,b}^{h_4}$  couplings, which are independent of the  $\varepsilon_i$  parameters. Another interesting decay mode of  $h_4$  is

$$h_4 \rightarrow W^+ H^- \quad (5.28)$$

if  $m_{h_4} > m_W + m_{H^-}$ . In the alignment limit, the coupling is given by

$$ig_{h_4 W^+ H^-}^\mu = -\frac{g}{2} (N_A - i\varepsilon_2) (p_{h_4} - p_{H^-})^\mu. \quad (5.29)$$

The decay mode has been studied in Refs. [40, 41], in the context of the CP-conserving 2HDM. It will become more important than the top-pair process when  $h_4$  is heavy since the decay width is proportional to  $m_{h_4}^3$ ,

$$\Gamma(h_4 \rightarrow W^+ H^-) = \frac{g^2(N_A^2 + \varepsilon_2^2)}{64\pi m_W^2} m_{h_4}^3 \lambda^{3/2} (1, m_{H^-}^2/m_{h_4}^2, m_W^2/m_{h_4}^2), \quad (5.30)$$

where  $\lambda(x, y, z) = (x - y - z)^2 - 4yz$ . Note that  $\varepsilon_2$  vanishes in the alignment limit and  $\tan\beta = 1$  as can be seen in Eq. (3.35). Therefore, the effect of the CP violation in the decay mode is only relevant when we depart from the alignment limit. Note that the same final state may appear from the decay of  $h_2$ . The coupling has the similar form as in (5.29). However, we should fix the charged Higgs mass as  $m_{H^+} = m_{h_2}$  or  $m_{H^+} = m_{h_4}$  to be consistent with the constraints from the electroweak precision [42–46]. By taking either choice, only one of the decay modes will be kinematically allowed. Due to the irreducible backgrounds of the  $t\bar{t}$  process in the SM, the sensitivity of the final state with  $W^+ H^-$  at the LHC turned out to be low [40]. Still, we expect that it will be possible to probe the decay mode at the High-Luminosity LHC and future collider experiments.

The other decay mode for the heavy Higgs bosons studied in Refs. [40, 41, 47] is  $h_i \rightarrow Zh_j$  for  $m_{h_i} > m_Z + m_{h_j}$ . The decay mode has already been searched by the ATLAS [48, 49] and CMS [50, 51] collaborations using the final state of  $\ell^+ \ell^- + b\bar{b}$ . The interpretation of experimental results for the CP-conserving 2HDM has been shown in Ref. [47]. In the alignment limit, the coupling for the  $h_4 \rightarrow Zh_1$  process is vanishing at leading order, while the coupling at the next-to-leading order is proportional to  $\varepsilon_i^2$ . The effects of the  $\varepsilon_i$  parameters for  $h_4 \rightarrow Zh_2$  also arise by the terms of the order of  $\varepsilon_i^2$ . Therefore, we find that the only relevant decay mode with the final state of  $Zh_j$  for the scenario with the pure singlet and the alignment limit is

$$h_2 \rightarrow Zh_1. \quad (5.31)$$

The coupling in the alignment limit is

$$ig_{h_1 h_2 Z}^\mu = -\frac{iN_A m_Z}{v} \varepsilon_1 (p_{h_2} - p_{h_1})^\mu, \quad (5.32)$$

and the decay width is proportional to  $m_{h_2}^3$ , similarly as in (5.30). Therefore, searching for  $h_2 \rightarrow Zh_1$  serves a direct probe of the  $\varepsilon_1$  parameter. The main background to this decay mode at the LHC is the  $Z$ -boson associated Higgs production,  $pp \rightarrow Z^* \rightarrow Zh_1$ , and the di-leptonic  $t\bar{t}$  process in the SM. We leave the detailed studies on the reach of the  $\varepsilon_1$  parameter using the  $h_2 \rightarrow Zh_1$  process at the LHC and future collider experiments, as our future publication. We stress that the other parameters,  $\varepsilon_2$  and  $\varepsilon_3$ , would become more relevant if we depart from the pure singlet scenario and the alignment limit.



## 6 The UV origins of CP violation

We discuss the origin of CP violating higher-dimensional operators in the effective potential. In particular, for generating the dimension-6 operator  $(SH_1^\dagger H_2)^2$ , which captures a physical CP violation, we introduce the NMSSM with  $U(1)'$  and two models with new doublet and singlet scalars or fermions.

### 6.1 Model A: The NMSSM with $U(1)'$ symmetry

We consider the NMSSM with  $U(1)'$  symmetry under which the singlet chiral superfield  $S$  is charged (Model A). The relevant interactions for the CP violation are given by

$$\mathcal{L}_{\text{Model A}} = -m_{\tilde{t}_L}^2 |\tilde{t}_L|^2 - m_{\tilde{t}_R}^2 |\tilde{t}_R|^2 - y_t A_t (H_1^0)^* \tilde{t}_L \tilde{t}_R^* - y_s A_s S H_1^\dagger H_2 + \text{h.c.} \quad (6.1)$$

where  $y_s$  is the Yukawa coupling between the singlet scalar and the Higgsinos in the superpotential,  $W = y_s S H_u H_d$ , with  $H_u = \tilde{H}_2$  and  $H_d = H_1$  in the basis of chiral superfields, and  $A_s, A_t$  are the trilinear soft mass terms. We note that  $y_s = -\mu/A_s$  in our model. Then, from the one-loop diagram with top squarks, we get the desired dimension-6 operator,  $(SH_1^\dagger H_2)^2$ , with as the following coefficient [52],

$$\frac{c_1}{\Lambda^2} = \frac{3y_t^4 y_s^2 A_t^2}{32\pi^2 (m_{\tilde{t}_1}^2 - m_{\tilde{t}_2}^2)^2} \mathcal{G}(m_{\tilde{t}_1}^2, m_{\tilde{t}_2}^2) \quad (6.2)$$

where  $m_{\tilde{t}_1}^2, m_{\tilde{t}_2}^2$  are the squared masses for top squarks, and the loop function  $\mathcal{G}$  is given by

$$\mathcal{G}(m_{\tilde{t}_1}^2, m_{\tilde{t}_2}^2) = 2 - \frac{m_{\tilde{t}_1}^2 + m_{\tilde{t}_2}^2}{m_{\tilde{t}_1}^2 - m_{\tilde{t}_2}^2} \ln \left( \frac{m_{\tilde{t}_1}^2}{m_{\tilde{t}_2}^2} \right). \quad (6.3)$$

For instance,  $m_{\tilde{t}_2}^2 \gg m_{\tilde{t}_1}^2 \gg |A_t| m_t$ , we can approximate Eq. (6.2) to

$$\frac{c_1}{\Lambda^2} \approx \frac{3y_t^4 y_s^2 A_t^2}{32\pi^2 m_{\tilde{t}_2}^4} \left[ 2 + \ln \left( \frac{m_{\tilde{t}_1}^2}{m_{\tilde{t}_2}^2} \right) \right]. \quad (6.4)$$

In this case, the nontrivial CP phase in the dimension-6 operator is originated from the CP phase in  $A_t$ .

In view of the eEDM constraints discussed for the cutoff scale in the previous section, we can impose  $\Lambda = 20\text{--}50$  TeV depending on the masses of heavy Higgs bosons, which can be translated to the bounds on the stop masses and mixing parameter. In Fig. 5, we show the parameter space for stop masses,  $m_{\tilde{t}_1}$  and  $m_{\tilde{t}_2}/m_{\tilde{t}_1}$ , which is ruled out by the eEDM bounds with the cutoff scale greater than 20, 50 TeV colored in gray and purple, respectively. Here, we have taken  $y_t = y_s = 1$ ,  $A_t = m_{\tilde{t}_1}$  and  $\text{Arg}(y_t^4 y_s^2 A_t^2) = \pi/2$ . Therefore, for degenerate masses for heavy Higgs bosons, for which the cutoff scale is constrained to be greater than 50 TeV, the lighter stop mass should be larger than up to 2 TeV (colored in purple in Fig. 5),

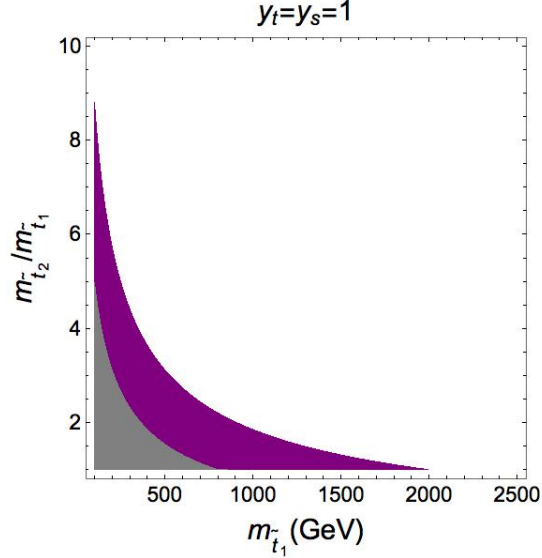


Figure 5: The parameter space for stop masses,  $m_{\tilde{t}_1}$  and  $m_{\tilde{t}_2}/m_{\tilde{t}_1}$ , with the eEDM constraints. We have set  $A_t = m_{\tilde{t}_1}$ ,  $y_t = y_s = 1$  and  $\text{Arg}(y_t^4 y_s^2 A_t^2) = \pi/2$ . The regions colored in gray and purple are ruled out by the eEDM bounds, for  $\Lambda/\sqrt{|c_I|} < 20, 50$  TeV, respectively.

depending on the mass of the heavier stop mass. As a result, we may probe the stop masses with the eEDM measurement beyond the reach of the LHC. On the other hand, for non-degenerate masses of heavy Higgs bosons, for which the cutoff scale is constrained to be as low as 20 TeV, the lighter stop mass up to 800 GeV (colored in gray in Fig. 5) is ruled out by the eEDM bound.

In the CP-violating NMSSM with CP violation from both tree- and loop-levels but with no  $U(1)'$ , we refer to Ref. [53] for a complete study on baryon asymmetry of the universe and electric dipole moment.

## 6.2 Model B: models with doublet and singlet scalars

Another example worth considering is the scalar dark matter as the origin of the CP violation (Model B). For this, we introduce an SM doublet  $\phi_D$  with hypercharge  $Y = +\frac{1}{2}$  and an SM singlet  $\phi_S$ , which are neutral under the  $U(1)'$  and the SM color. We also impose the global symmetry,  $U(1)_R$ , under which  $S$  carries charge +2,  $\phi_D, \phi_S$  carry charge +1 whereas two Higgs doublets and the SM fermions are neutral, as shown in Table 2. The  $U(1)_R$  symmetry corresponds to the one in the supersymmetric models as in Model A where the  $A$ -term breaks the  $U(1)_R$  symmetry softly.

In this setup, we introduce the couplings between the extra scalars and  $S, H_{1,2}$ , as in the following Lagrangian,

$$\mathcal{L}_{\text{Model B}} = -m_D^2 |\phi_D|^2 - m_S^2 |\phi_S|^2 - \lambda_D S H_2 \phi_D^\dagger \phi_S^* - A_D H_1^\dagger \phi_D \phi_S + \text{h.c.}, \quad (6.5)$$

where  $A_D$  is the spurion parameter carrying charge  $-2$  under the  $U(1)_R$ . The  $U(1)_R$  symme-

try is softly broken to  $Z_2$  due to the  $A_D$  term as well as the  $\mu$  term. Then, since  $\phi_D$  and  $\phi_S$  are  $Z_2$  odd, the lighter neutral complex scalar among them can be a dark matter candidate. Then, similarly to the previous example, from the loops with new scalars, we can obtain the dimension-6 operator  $(SH_1^\dagger H_2)^2$ , with the coefficient,  $\frac{c_1}{\Lambda^2} \sim \frac{\lambda_D^2 A_D^2}{16\pi^2 m_D^4}$  for  $m_D \gg m_S \gg A_D v_1$ . In this case, the nontrivial CP phase in the dimension-6 operator stems from the CP phase of the coupling to the dark scalars  $A_D$ .

	$S$	$H_1$	$H_2$	$\phi_S$	$\phi_D$	$A_D$
$Q'$	$\frac{1}{3}x$	0	$-\frac{1}{3}x$	0	0	0
$U(1)_R$	+2	0	0	+1	+1	-2

Table 2:  $U(1)'$  and  $U(1)_R$  charges of scalars for Model B.

In this case, there are similar bounds on the masses for doublet and singlet scalars,  $m_D$  and  $m_S$ , similarly as in the NMSSM with  $U(1)'$ , if we identify  $\lambda_D = y_t^2 y_s$  and  $A_D \sim A_t \sim m_S$ . The difference from the NMSSM with  $U(1)'$  is that new particles running in the loops contain charge-neutral scalars, the lighter of which can be a dark matter candidate, that is,  $\phi_S$ , unlike the stops. Therefore, it would be interesting to pursue the details on the interplay between the eEDM bound and the CP violation in the dark sector.

### 6.3 Model C: models with doublet and singlet fermions

We also consider the possibility of fermion dark matter for the CP violation (Model C). We introduce a vector-like doublet fermion, composed of  $\psi, \tilde{\psi}$ , with hypercharge  $Y = -\frac{1}{2}, +\frac{1}{2}$ , and a Weyl singlet fermion  $\psi'$ , that are neutral under the  $U(1)'$ , and a vector-like singlet fermion, composed of  $\chi, \tilde{\chi}$ , which carry charges  $-\frac{1}{3}x, +\frac{1}{3}x$  under the  $U(1)'$ . We also assign the charges for scalars and two-component spinors under the global  $U(1)_R$  symmetry as in Table 3. Thus, as in the previous models, the  $U(1)_R$  is softly broken to  $Z_2$  by the  $\mu$  term and the Dirac mass term for  $\chi, \tilde{\chi}$ . Then, the lightest neutral fermion among the extra neutral fermions, which are  $Z_2$  odd, can be a dark matter candidate.

Then, the Lagrangian for the extra fermions is, in the two-component spinor notations, given by

$$\mathcal{L}_{\text{Model C}} = -m_\psi \psi \tilde{\psi} - m_\chi \chi^\dagger \tilde{\chi}^\dagger - \lambda_S S \psi' \chi - y_1 \tilde{H}_1 \psi^\dagger \psi'^\dagger - y_2 H_2 \tilde{\chi} \psi + \text{h.c.}, \quad (6.6)$$

where  $m_\chi$  is the spurion mass parameter carrying charge  $-2$  under the  $U(1)_R$ . Then, due to the loops with extra fermions, the dimension-6 operator  $(SH_1^\dagger H_2)^2$  is generated with the coefficient,  $\frac{c_1}{\Lambda^2} \sim \frac{\lambda_S^2 y_1^2 y_2^2 m_\chi^2}{16\pi^2 m_\psi^4}$ . In this case, the nontrivial CP phase in the dimension-6 operator is from the CP phases of the Yukawa couplings to the extra fermions and/or the Dirac mass

	$S$	$H_1$	$H_2$	$\psi'$	$\psi$	$\tilde{\psi}$	$\chi$	$\tilde{\chi}$
$Q'$	$\frac{1}{3}x$	0	$-\frac{1}{3}x$	0	0	0	$-\frac{1}{3}x$	$+\frac{1}{3}x$
$U(1)_R$	+2	0	0	-1	+1	-1	-1	-1

Table 3:  $U(1)'$  and  $U(1)_R$  charges of scalars and extra fermions for Model C.

term, and it can be sufficiently suppressed for  $m_\psi \gg m_\chi$  with Yukawa couplings,  $\lambda_S, y_{1,2}$ , being of order one.

In this case, as compared to the case in the NMSSM with  $U(1)'$ , the role of dimensionless couplings is played by  $\lambda_S y_1 y_2 = y_t^2 y_s$  and the dimensionful parameter is translated to  $m_\chi \sim A_t$ . Then, the smallness of the CP-violating dimension-6 operator is attributed to a small  $U(1)_R$  breaking mass term for  $\chi$  and  $\tilde{\chi}$ . While the  $\psi, \tilde{\psi}$  and  $\psi', \chi$  pairs have large Dirac masses,  $\tilde{\chi}$ , having a Majorana fermion with a small mass, is a candidate for dark matter. We postpone the detail analysis of the model in a future publication.

## 7 Conclusions

We have presented a model-independent parametrization of the CP violation in the effective theory for the 2HDM with a local  $U(1)'$  and showed how the higher dimensional operators in the scalar potential violate the CP symmetry at the observable level. The tadpole condition from the minimization of the scalar potential renders the mixing Higgs mass parameter carrying a nonzero CP phase by the interplay with the higher dimensional operators. We calculated the electric dipole moment of the electron at two loops due to the mixings between CP-even and CP-odd scalars in our model and identified the minimum cutoff scale from the bound on eEDM to be 20–50 TeV, depending on the mass spectrum of heavy Higgs bosons.

We also showed how the inputs from the collider searches for heavy Higgs bosons with CP violation can be used to make an independent test of the CP-violating parameters in the models. In particular, in the alignment limit favored by the Higgs data, the pseudoscalar-like scalar can also decay into  $WW$  or  $ZZ$ , and it has the  $W^+H^-$  decay mode modified due to the CP-violating mixing parameters, which might be testable at the High-Luminosity LHC. Furthermore, the  $h_2 \rightarrow Zh_1$  process with  $\ell^+\ell^- + b\bar{b}$  final states at the LHC and future collider experiments can serve a direct probe of the CP-violating parameter against the backgrounds coming from the  $Z$ -boson associated production of  $h_1$  or the di-leptons from  $t\bar{t}$ .

We have also discussed the microscopic origins for generating the higher-dimensional operators in the scalar potential, in the context of both supersymmetric or non-supersymmetric models. In the case of the NMSSM with  $U(1)'$ , the mass parameters of stops running in loops can generate the CP-violating dimension-6 operator in the scalar potential, thus they can be

constrained indirectly by the eEDM according to our general results. Depending on whether the heavy Higgs bosons have split masses or not, the eEDM bound can constrain the lighter stop mass to be heavier than up to 800 GeV–2 TeV, thus being complementary to the direct searches for stops at the High-Luminosity LHC and future colliders. In models with new neutral scalars or fermions running in loops, the lighter neutral particle is a good candidate for dark matter with CP-violating couplings, so there can be a variety of ways of probing the CP violation by dark matter experiments as well as more precise measurements of eEDM such as ACMEIII.

Finally we remark that in CP-violating 2HDMs, there is a tension between the strong signal for gravitational waves and the electroweak baryogenesis [54, 55]. We leave the possibility of addressing the baryon asymmetry of the Universe in microscopic models with  $U(1)'$  to a future study.

## Acknowledgments

The work of LB is supported by the National Natural Science Foundation of China under grant No.11605016 and No.11947406. The work of HML is supported in part by Basic Science Research Program through the National Research Foundation of Korea (NRF) funded by the Ministry of Education, Science and Technology (NRF-2019R1A2C2003738 and NRF-2018R1A4A1025334). CBP is supported by IBS under the project code, IBS-R018-D1.

## Appendix A The minimization and tadpole conditions

For the scalar potential with phase-rotated scalar fields in eqs. (3.2)-(3.4) and redefined parameters in eqs. (3.5)-(3.11), the minimization conditions yield

$$\begin{aligned} \mu_1^2 &= \frac{1}{\sqrt{2}} \operatorname{Re}(\mu) \frac{v_2 v_s}{v_1} - \lambda_1 v_1^2 - (\lambda_3 + \lambda_4) v_2^2 - \kappa_1 v_s^2 + \sum_{a=1}^3 \beta_{a1} \omega_a^2 \\ &\quad - \frac{1}{2\Lambda^2} \operatorname{Re}(c_1) v_2^2 v_s^2 - \frac{1}{2\Lambda^2} \operatorname{Re}(c_2) v_2^2 v_s \omega_3, \end{aligned} \quad (\text{A.1})$$

$$\begin{aligned} \mu_2^2 &= \frac{1}{\sqrt{2}} \operatorname{Re}(\mu) \frac{v_1 v_s}{v_2} - \lambda_2 v_2^2 - (\lambda_3 + \lambda_4) v_1^2 - \kappa_2 v_s^2 + \sum_{a=1}^3 \beta_{a2} \omega_a^2 \\ &\quad - \frac{1}{2\Lambda^2} \operatorname{Re}(c_1) v_1^2 v_s^2 - \frac{1}{2\Lambda^2} \operatorname{Re}(c_2) v_1^2 v_s \omega_3, \end{aligned} \quad (\text{A.2})$$

$$\begin{aligned} m_S^2 &= \frac{1}{\sqrt{2}} \operatorname{Re}(\mu) \frac{v_1 v_2}{v_s} - \lambda_S v_s^2 - \kappa_1 v_1^2 - \kappa_2 v_2^2 - \sum_{a=1}^3 \beta_{a3} \omega_a^2 - \frac{3}{2} \operatorname{Re}(\rho) v_s \omega_3 \\ &\quad - \frac{3}{2\sqrt{2}\Lambda} \operatorname{Re}(d_1) v_s \omega_1 \omega_2 - \frac{1}{2\Lambda^2} \operatorname{Re}(c_1) v_1^2 v_2^2 - \frac{1}{4\Lambda^2} \operatorname{Re}(c_2) \frac{v_1^2 v_2^2 \omega_3}{v_s}, \end{aligned} \quad (\text{A.3})$$

$$\begin{aligned}\mu_{\Phi_1}^2 &= -\frac{1}{\sqrt{2}} \operatorname{Re}(\mu_\Phi) \frac{\omega_2 \omega_3}{\omega_1} - \lambda_{\Phi_1} \omega_1^2 - (\beta_{11} v_1^2 + \beta_{12} v_2^2 + \beta_{13} v_s^2) - \lambda_{12} \omega_2^2 - \lambda_{13} \omega_3^2 \\ &\quad - \frac{1}{2\sqrt{2}\Lambda} \operatorname{Re}(d_1) \frac{v_s^3 \omega_2}{\omega_1} - \frac{1}{2\Lambda^2} \operatorname{Re}(d_2) \omega_2^2 \omega_3^2,\end{aligned}\tag{A.4}$$

$$\begin{aligned}\mu_{\Phi_2}^2 &= -\frac{1}{\sqrt{2}} \operatorname{Re}(\mu_\Phi) \frac{\omega_1 \omega_3}{\omega_2} - \lambda_{\Phi_2} \omega_2^2 - (\beta_{21} v_1^2 + \beta_{22} v_2^2 + \beta_{23} v_s^2) - \lambda_{12} \omega_1^2 - \lambda_{23} \omega_3^2 \\ &\quad - \frac{1}{2\sqrt{2}\Lambda} \operatorname{Re}(d_1) \frac{v_s^3 \omega_1}{\omega_2} - \frac{1}{2\Lambda^2} \operatorname{Re}(d_2) \omega_1^2 \omega_3^2,\end{aligned}\tag{A.5}$$

$$\begin{aligned}\mu_{\Phi_3}^2 &= -\frac{1}{2} \operatorname{Re}(\rho) \frac{v_s^3}{\omega_3} - \frac{1}{\sqrt{2}} \operatorname{Re}(\mu_\Phi) \frac{\omega_1 \omega_2}{\omega_3} - \lambda_{\Phi_2} \omega_3^2 \\ &\quad - (\beta_{31} v_1^2 + \beta_{32} v_2^2 + \beta_{33} v_s^2) - \lambda_{13} \omega_1^2 - \lambda_{23} \omega_2^2 \\ &\quad - \frac{1}{4\Lambda^2} \operatorname{Re}(c_2) \frac{v_1^2 v_2^2 v_s}{\omega_3} - \frac{1}{2\Lambda^2} \operatorname{Re}(d_2) \omega_1^2 \omega_2^2.\end{aligned}\tag{A.6}$$

The tadpole parameters for the pseudoscalar fields are given by

$$\frac{T_{\eta_1}}{v_2} = -\frac{T_{\eta_2}}{v_1} = -\frac{1}{\sqrt{2}} \operatorname{Im}(\mu) v_s + \frac{1}{2\Lambda^2} \operatorname{Im}(c_1) v_1 v_2 v_s^2 + \frac{1}{2\Lambda^2} \operatorname{Im}(c_2) v_1 v_2 v_s \omega_3,\tag{A.7}$$

$$\begin{aligned}\frac{T_{\eta_S}}{v_s} &= \frac{1}{\sqrt{2}} \operatorname{Im}(\mu) \frac{v_1 v_2}{v_s} - \frac{3}{2} \operatorname{Im}(\rho) v_s \omega_3 - \frac{3}{2\sqrt{2}\Lambda} \operatorname{Im}(d_1) v_s \omega_1 \omega_2 \\ &\quad - \frac{1}{2\Lambda^2} \operatorname{Im}(c_1) v_1^2 v_2^2 + \frac{1}{4\Lambda^2} \operatorname{Im}(c_2) \frac{v_1^2 v_2^2 \omega_3}{v_s},\end{aligned}\tag{A.8}$$

$$\frac{T_{\Phi_{1I}}}{\omega_2} = \frac{T_{\Phi_{2I}}}{\omega_1} = -\frac{1}{\sqrt{2}} \operatorname{Im}(\mu_\Phi) \omega_3 - \frac{1}{2\sqrt{2}\Lambda} \operatorname{Im}(d_1) v_s^3 - \frac{1}{2\Lambda^2} \operatorname{Im}(d_2) \omega_1 \omega_2 \omega_3^2,\tag{A.9}$$

$$\begin{aligned}\frac{T_{\Phi_{3I}}}{\omega_3} &= \frac{1}{\sqrt{2}} \operatorname{Im}(\mu_\Phi) \frac{\omega_1 \omega_2}{\omega_3} + \frac{1}{2} \operatorname{Im}(\rho) \frac{v_s^3}{\omega_3} \\ &\quad - \frac{1}{4\Lambda^2} \operatorname{Im}(c_2) \frac{v_1^2 v_2^2 v_s}{\omega_3} + \frac{1}{2\Lambda^2} \operatorname{Im}(d_2) \omega_1^2 \omega_2^2.\end{aligned}\tag{A.10}$$

By combining the above relations, we have

$$\begin{aligned}0 &= \frac{v_1 v_2}{v_s^3} \frac{T_{\eta_1}}{v_2} + \frac{T_{\eta_S}}{v_s} + \frac{3\omega_1 \omega_2}{v_s^2} \frac{T_{\Phi_{1I}}}{\omega_2} + \frac{3\omega_3^2}{v_s^2} \frac{T_{\Phi_{3I}}}{\omega_3} \\ &= -\frac{3}{\sqrt{2}\Lambda} \operatorname{Im}(d_1) v_s \omega_1 \omega_2,\end{aligned}\tag{A.11}$$

so  $\operatorname{Im}(d_1) = 0$ . Then, we further find that

$$\begin{aligned}0 &= \frac{v_1 v_2}{3v_s^3} \frac{T_{\eta_1}}{v_2} + \frac{1}{3} \frac{T_{\eta_S}}{v_s} \\ &= -\frac{1}{2} \operatorname{Im}(\rho) v_s \omega_3 + \frac{1}{4\Lambda^2} \operatorname{Im}(c_2) \frac{v_1^2 v_2^2 \omega_3}{v_s},\end{aligned}\tag{A.12}$$

which results in  $\operatorname{Im}(\rho) = \operatorname{Im}(c_2) = 0$ . The remaining combinations are

$$0 = \left. \frac{T_{\eta_1}}{v_2} \right|_{\operatorname{Im}(c_2)=0}$$

$$= -\frac{1}{\sqrt{2}} \text{Im}(\mu)v_s + \frac{1}{2\Lambda^2} \text{Im}(c_1)v_1v_2v_s^2, \quad (\text{A.13})$$

$$0 = \left. \frac{T_{\Phi_{1I}}}{\omega_2} \right|_{\text{Im}(d_1)=0} = -\frac{1}{\sqrt{2}} \text{Im}(\mu_\Phi)\omega_3 - \frac{1}{2\Lambda^2} \text{Im}(d_2)\omega_1\omega_2\omega_3^2. \quad (\text{A.14})$$

Consequently, the tadpole conditions in eqs. (A.13) and (A.14) determine the CP phases of the mass parameters,  $\mu$  and  $\mu_\Phi$ , in terms of the CP phases of the dimension-6 operators,  $c_1$  and  $d_2$ , respectively. In the text, we used the results focusing on  $c_1$  in order to see the CP violating mixings between CP-even and CP-odd scalars in two Higgs doublet models with  $U(1)'$ .

## Appendix B Diagonalization of scalar mass matrices

In the absence of the CP violation, the would-be Goldstone bosons,  $G_Y$  and  $G'$ , for the spontaneously broken  $U(1)_Y \times U(1)'$ , can be identified as follows,

$$G_Y = \frac{2}{v} \left( \frac{1}{2}v_1\eta_1 + \frac{1}{2}v_2\eta_2 \right) = \cos \beta \eta_1 + \sin \beta \eta_2, \quad (\text{B.1})$$

$$G' = \frac{3}{xv_{Z'}} \left( \frac{1}{3}xv_s S_I - \frac{1}{3}xv_2\eta_2 \right) = \frac{1}{v_{Z'}} \left( v_s S_I - v \sin \beta \eta_2 \right), \quad (\text{B.2})$$

with  $v^2 = v_1^2 + v_2^2$  and  $v_{Z'}^2 \equiv v_s^2 + v_2^2$ . Here, we note that the  $Z'$  gauge boson is given by  $m_{Z'} \simeq \frac{1}{3}xg_{Z'}v_{Z'}$  if the extra singlet VEVs from  $\Phi_a$  are small. Then, the heavy pseudoscalar  $A^0$  can be taken to be orthogonal to the above two would-be Goldstone bosons as

$$A^0 = N_A \left( \sin \beta \eta_1 - \cos \beta \eta_2 - \frac{v}{v_s} \sin \beta \cos \beta S_I \right) \quad (\text{B.3})$$

with  $N_A$  given in (3.21). Therefore, we now make a transformation to the basis with would-be Goldstone bosons,  $G_Y$  and  $G'$ , and the heavy pseudoscalar  $A^0$ , by

$$\begin{pmatrix} \eta_1 \\ \eta_2 \\ S_I \end{pmatrix} = \mathcal{R}_3 \begin{pmatrix} A^0 \\ G_Y \\ G' \end{pmatrix}, \quad (\text{B.4})$$

where  $\mathcal{R}_3$  is the  $3 \times 3$  transformation matrix and its inverse reads from Eqs. (B.1), (B.2) and (B.3), as follows,

$$\mathcal{R}_3 = \begin{pmatrix} \frac{N_A v_2}{v} & -\frac{N_A v_1}{v} & -\frac{N_A v_1 v_2}{v v_s} \\ \frac{v_1}{v} & \frac{v_2}{v} & 0 \\ 0 & -\frac{v_2}{v_{Z'}} & \frac{v_s}{v_{Z'}} \end{pmatrix}^{-1}. \quad (\text{B.5})$$

Then, we find that  $G_Y$  and  $G'$  appear massless as expected, and  $A^0$  mixes with the CP-even scalars due to CP violation. The results are used to choose the basis for the squared mass matrix for scalars with CP violation in the text.

We note from Eq. (B.4) that the CP-odd scalars can be expressed in terms of the CP-odd scalar  $A^0$  and the would-be Goldstone bosons as follows.

$$\eta_1 = N_A \left( \sin \beta A^0 + \frac{N_A v_{Z'}}{v_s^2} \cos \beta G_Y + \frac{N_A v v_{Z'}}{v_s^2} \cos \beta \sin^2 \beta G' \right), \quad (\text{B.6})$$

$$\eta_2 = N_A \left( -\cos \beta A^0 + N_A \sin \beta G_Y - \frac{N_A v v_{Z'}}{v_s^2} \cos^2 \beta \sin \beta G' \right), \quad (\text{B.7})$$

$$S_I = N_A \left( -\frac{v}{v_s} \sin \beta \cos \beta A^0 + \frac{N_A v}{v_s} \sin^2 \beta G_Y + \frac{N_A v_{Z'}}{v_s} G' \right). \quad (\text{B.8})$$

Following the procedure in Ref. [11], we can diagonalize the  $3 \times 3$  sub-matrix for CP-even scalars in the  $4 \times 4$  mass matrix in Eq. (3.17) as

$$R_h M_{3 \times 3}^2 R_h^T = \text{diag}(m_{h_1^0}^2, m_{h_2^0}^2, m_{h_3^0}^2), \quad (\text{B.9})$$

with the rotation matrix,

$$R_h = \begin{pmatrix} c_{\alpha_1} c_{\alpha_2} & s_{\alpha_1} c_{\alpha_2} & s_{\alpha_2} \\ -(c_{\alpha_1} s_{\alpha_2} s_{\alpha_3} + s_{\alpha_1} c_{\alpha_3}) & c_{\alpha_1} c_{\alpha_3} - s_{\alpha_1} s_{\alpha_2} s_{\alpha_3} & c_{\alpha_2} s_{\alpha_3} \\ -c_{\alpha_1} s_{\alpha_2} c_{\alpha_3} + s_{\alpha_1} s_{\alpha_3} & -(c_{\alpha_1} s_{\alpha_3} + s_{\alpha_1} s_{\alpha_2} c_{\alpha_3}) & c_{\alpha_2} c_{\alpha_3} \end{pmatrix}, \quad (\text{B.10})$$

where  $s_{\alpha_i} \equiv \sin \alpha_i$  and  $c_{\alpha_i} \equiv \cos \alpha_i$ , with  $-\pi/2 \leq \alpha_{1,2,3} < \pi/2$ . Then, the mass eigenvalues of CP-even scalars are given by

$$\begin{aligned} m_{h_1^0}^2 &= \frac{1}{2}(a + b - \sqrt{D}) \equiv m_h^2, \\ m_{h_2^0}^2 &= \frac{1}{2}(a + b + \sqrt{D}) \equiv m_H^2, \\ m_{h_3^0}^2 &= 2\lambda_S v_s^2 + \frac{\mu v_1 v_2}{\sqrt{2} v_s} \equiv m_s^2, \end{aligned} \quad (\text{B.11})$$

where

$$a \equiv 2\lambda_1 v_1^2 + \frac{\mu_R v_2 v_s}{\sqrt{2} v_1}, \quad b \equiv 2\lambda_2 v_2^2 + \frac{\mu_R v_1 v_s}{\sqrt{2} v_2}, \quad D \equiv (a - b)^2 + 4d^2, \quad (\text{B.12})$$

with  $d \equiv 2v_1 v_2 (\lambda_3 + \lambda_4) + \frac{c_R}{\Lambda^2} v_1 v_2 v_s^2 - \frac{1}{\sqrt{2}} \mu_R v_s$ . We also denote with  $h_4^0 \equiv A^0$  that

$$m_{h_4^0}^2 \equiv m_{A^0}^2 = \frac{v^2 v_s}{\sqrt{2} v_1 v_2} \left( \mu_R - \frac{\sqrt{2} c_R v_1 v_2 v_s}{\Lambda^2} \right) N_A^{-2}. \quad (\text{B.13})$$

The above results are used for the approximate mass eigenstates in the text.

The charged Goldstone boson  $G^+$  and charged Higgs scalar  $H^+$  identified as

$$\begin{aligned} G^+ &= \cos \beta \phi_1^+ + \sin \beta \phi_2^+, \\ H^+ &= \sin \beta \phi_1^+ - \cos \beta \phi_2^+ \end{aligned} \quad (\text{B.14})$$

with nonzero mass eigenvalue given by

$$m_{H^+}^2 = m_A^2 - \left( \frac{\mu \sin \beta \cos \beta}{\sqrt{2} v_s} + \lambda_4 \right) v^2. \quad (\text{B.15})$$



## Appendix C Self-interactions and gauge interactions for scalar fields

The couplings for the Higgs self-interactions associated with the charged Higgs boson are

$$\begin{aligned}
g_{H^+H^-h_1} &= (\lambda_1 c_\alpha s_\beta + \lambda_2 s_\alpha c_\beta) v s_{2\beta} + 2\lambda_3 v c_{\beta-\alpha} \\
&\quad - \left( \lambda_3 + \lambda_4 + \frac{c_R}{2\Lambda^2} v_s^2 \right) v s_{\beta+\alpha} s_{2\beta} - \frac{\sqrt{2}\mu_I v_s \varepsilon_1}{N_A v}, \\
g_{H^+H^-h_2} &= -(\lambda_1 s_\alpha s_\beta - \lambda_2 c_\alpha c_\beta) v s_{2\beta} + 2\lambda_3 v s_{\beta-\alpha} \\
&\quad - \left( \lambda_3 + \lambda_4 + \frac{c_R}{2\Lambda^2} v_s^2 \right) v c_{\beta+\alpha} s_{2\beta} - \frac{\sqrt{2}\mu_I v_s \varepsilon_2}{N_A v}, \\
g_{H^+H^-h_3} &= \frac{1}{\sqrt{2}} \mu_R s_{2\beta} + 2(\kappa_1 s_\beta^2 + \kappa_2 c_\beta^2) v_s - \frac{c_R}{2\Lambda^2} v^2 v_s s_{2\beta}^2 - \frac{\sqrt{2}\mu_I v_s \varepsilon_3}{N_A v}, \\
g_{H^+H^-h_4} &= [\lambda_1 s_\beta (-c_\alpha \varepsilon_1 + s_\alpha \varepsilon_2) + \lambda_2 c_\beta (-s_\alpha \varepsilon_1 - c_\alpha \varepsilon_2)] v s_{2\beta} \\
&\quad - 2\lambda_3 (c_{\beta-\alpha} \varepsilon_1 + s_{\beta-\alpha} \varepsilon_2) v + \left( \lambda_3 + \lambda_4 + \frac{c_R}{2\Lambda^2} v_s^2 \right) (s_{\beta+\alpha} \varepsilon_1 + c_{\beta+\alpha} \varepsilon_2) v s_{2\beta} \\
&\quad - \left[ \frac{1}{\sqrt{2}} \mu_R s_{2\beta} + 2(\kappa_1 s_\beta^2 + \kappa_2 c_\beta^2) v_s - \frac{c_R}{2\Lambda^2} s_{2\beta}^2 v^2 v_s \right] \varepsilon_3 - \frac{\sqrt{2}\mu_I v_s}{N_A v} \\
&= -g_{H^+H^-h_1} \varepsilon_1 - g_{H^+H^-h_2} \varepsilon_2 - g_{H^+H^-h_3} \varepsilon_3 - \frac{\sqrt{2}\mu_I v_s}{N_A v} + \mathcal{O}(\varepsilon_i^2). \tag{C.1}
\end{aligned}$$

The quartic couplings can be expressed by the Higgs masses and mixing angles:

$$\begin{aligned}
\lambda_1 &= \frac{2 \sum_i m_{h_i^0}^2 (R_h)_{i1}^2 - \sqrt{2}\mu_R v_s t_\beta}{4v^2 c_\beta^2} \approx \frac{2(m_{h_1^0}^2 c_\alpha^2 + m_{h_2^0}^2 s_\alpha^2) - \sqrt{2}\mu_R v_s t_\beta}{4v^2 c_\beta^2}, \\
\lambda_2 &= \frac{2 \sum_i m_{h_i^0}^2 (R_h)_{i2}^2 - \sqrt{2}\mu_R v_s / t_\beta}{4v^2 s_\beta^2} \approx \frac{2(m_{h_1^0}^2 s_\alpha^2 + m_{h_2^0}^2 c_\alpha^2) - \sqrt{2}\mu_R v_s / t_\beta}{4v^2 s_\beta^2}, \\
\lambda_3 + \lambda_4 + \frac{c_R}{2\Lambda^2} v_s^2 &= \frac{\sqrt{2}\mu_R v_s + 2 \sum_i m_{h_i^0}^2 (R_h)_{i1} (R_h)_{i2}}{2v^2 s_{2\beta}} \approx \frac{\sqrt{2}\mu_R v_s + (m_{h_1^0}^2 - m_{h_2^0}^2) s_{2\alpha}}{2v^2 s_{2\beta}}, \\
\lambda_4 &= -\frac{m_{H^+}^2}{v^2} + \frac{\mu_R v_s}{\sqrt{2} s_\beta c_\beta v^2} - \frac{c_R}{\Lambda^2} \frac{v_s^2}{N_A^2} \\
\lambda_3 &= \frac{\sqrt{2}\mu_R v_s + 2 \sum_i m_{h_i^0}^2 (R_h)_{i1} (R_h)_{i2}}{2v^2 s_{2\beta}} - \lambda_4 - \frac{c_R}{2\Lambda^2} v_s^2 \\
&\approx \frac{m_{H^+}^2}{v^2} + \frac{s_{2\alpha}}{2s_{2\beta}} \frac{m_{h_1^0}^2 - m_{h_2^0}^2}{v^2} - \frac{\mu_R v_s}{\sqrt{2} s_{2\beta} v^2} + \frac{c_R}{2\Lambda^2} (v_s^2 + 2v^2 s_\beta^2 c_\beta^2), \\
\kappa_1 + \frac{c_R}{2\Lambda^2} v^2 s_\beta^2 &= \frac{\sqrt{2}\mu_R v s_\beta + 2 \sum_i m_{h_i^0}^2 (R_h)_{i1} (R_h)_{i3}}{4v v_s c_\beta} \approx \frac{\mu_R s_\beta}{2\sqrt{2} v_s c_\beta}, \\
\kappa_2 + \frac{c_R}{2\Lambda^2} v^2 c_\beta^2 &= \frac{\sqrt{2}\mu_R v c_\beta + 2 \sum_i m_{h_i^0}^2 (R_h)_{i2} (R_h)_{i3}}{4v v_s s_\beta} \approx \frac{\mu_R c_\beta}{2\sqrt{2} v_s s_\beta}. \tag{C.2}
\end{aligned}$$

Here we have taken the limit where the mixing with the singlet field is negligible. Using the relations in the above, the Higgs couplings are now given as

$$g_{H^+H^-h_1} \approx c_{\beta-\alpha} \frac{2m_{H^+}^2}{v} + \left( \frac{s_\alpha c_\beta^2}{s_\beta} + \frac{c_\alpha s_\beta^2}{c_\beta} \right) \frac{m_{h_1^0}^2}{v} - \frac{\mu_R v_s s_{\beta+\alpha}}{\sqrt{2} v s_\beta^2 c_\beta^2} - \frac{\sqrt{2} \mu_I v_s \varepsilon_1}{N_A v} + \frac{c_R}{\Lambda^2} v (v_s^2 + 2v^2 s_\beta^2 c_\beta^2) c_{\beta-\alpha}, \quad (\text{C.3})$$

$$g_{H^+H^-h_2} \approx s_{\beta-\alpha} \frac{2m_{H^+}^2}{v} + \left( \frac{c_\alpha c_\beta^2}{s_\beta} - \frac{s_\alpha s_\beta^2}{c_\beta} \right) \frac{m_{h_2^0}^2}{v} - \frac{\mu_R v_s c_{\beta+\alpha}}{\sqrt{2} v s_\beta^2 c_\beta^2} - \frac{\sqrt{2} \mu_I v_s \varepsilon_2}{N_A v} + \frac{c_R}{\Lambda^2} v (v_s^2 + 2v^2 s_\beta^2 c_\beta^2) s_{\beta-\alpha}, \quad (\text{C.4})$$

$$g_{H^+H^-h_3} \approx \frac{\mu_R}{\sqrt{2} s_\beta c_\beta} - \frac{\sqrt{2} \mu_I v_s \varepsilon_3}{N_A v} - \frac{c_R}{\Lambda^2} v^2 v_s, \quad (\text{C.5})$$

$$g_{H^+H^-h_4} \approx -g_{H^+H^-h_1} \varepsilon_1 - g_{H^+H^-h_2} \varepsilon_2 - g_{H^+H^-h_3} \varepsilon_3 - \frac{\sqrt{2} \mu_I v_s}{N_A v}. \quad (\text{C.6})$$

The Higgs interactions to the  $W$  bosons arise through the kinetic terms.

$$\begin{aligned} \mathcal{L}_K &= |D_\mu H_1|^2 + |D_\mu H_2|^2 \\ &\supset \frac{g^2 v}{2} (c_\beta \rho_1 + s_\beta \rho_2) W_\mu^+ W^{-\mu} + \left[ \frac{ig}{2} W_\mu^+ (\phi_1^- \partial^\mu \rho_1 - \rho_1 \partial^\mu \phi_1^- + \phi_2^- \partial^\mu \rho_2 - \rho_2 \partial^\mu \phi_2^-) \right. \\ &\quad \left. - \frac{g}{2} W_\mu^+ (\phi_1^- \partial^\mu \eta_1 - \eta_1 \partial^\mu \phi_1^- + \phi_2^- \partial^\mu \eta_2 - \eta_2 \partial^\mu \phi_2^-) + \text{c.c.} \right] \\ &\approx \frac{2m_W^2}{v} \left[ c_{\beta-\alpha} h_1 + s_{\beta-\alpha} h_2 - (c_{\beta-\alpha} \varepsilon_1 + s_{\beta-\alpha} \varepsilon_2) h_4 \right] W_\mu^+ W^{-\mu} \\ &\quad + \left[ \frac{ig(s_{\beta-\alpha} + iN_A \varepsilon_1)}{2} W_\mu^+ (H^- \partial^\mu h_1 - h_1 \partial^\mu H^-) \right. \\ &\quad - \frac{ig(c_{\beta-\alpha} - iN_A \varepsilon_2)}{2} W_\mu^+ (H^- \partial^\mu h_2 - h_2 \partial^\mu H^-) \\ &\quad - \frac{gN_A \varepsilon_3}{2} W_\mu^+ (H^- \partial^\mu h_3 - h_3 \partial^\mu H^-) \\ &\quad \left. - \frac{ig(s_{\beta-\alpha} \varepsilon_1 - c_{\beta-\alpha} \varepsilon_2 - iN_A)}{2} W_\mu^+ (H^- \partial^\mu h_4 - h_4 \partial^\mu H^-) + \text{c.c.} \right]. \quad (\text{C.7}) \end{aligned}$$

Note that the charged Higgs boson interacts with the neutral Higgs and  $W$  bosons through derivative couplings. The couplings are

$$\begin{aligned} ig_{h_1 W^\pm H^\mp}^\mu &= -\frac{g}{2} (N_A \varepsilon_1 \mp i s_{\beta-\alpha}) (p_{h_1} - p_{H^\pm})^\mu, \\ ig_{h_2 W^\pm H^\mp}^\mu &= -\frac{g}{2} (N_A \varepsilon_2 \pm i c_{\beta-\alpha}) (p_{h_2} - p_{H^\pm})^\mu, \\ ig_{h_3 W^\pm H^\mp}^\mu &= -\frac{gN_A \varepsilon_3}{2} (p_{h_3} - p_{H^\pm})^\mu, \end{aligned}$$

$$ig_{h_4 W^\pm H^\mp}^\mu = -\frac{g}{2} \left[ N_A \pm i \left( s_{\beta-\alpha} \varepsilon_1 - c_{\beta-\alpha} \varepsilon_2 \right) \right] (p_{h_4} - p_{H^\pm})^\mu. \quad (\text{C.8})$$

Here all the momenta  $p_{h_i}$  and  $p_{H^\pm}$  are all *incoming* to the vertices.

Similarly, the Higgs interactions to the  $Z$  bosons are given from the following terms,

$$\begin{aligned} \mathcal{L}_K \supset & \frac{m_Z^2}{2v^2} \left[ (v_1 + \rho_1)^2 + (v_2 + \rho_2)^2 \right] Z_\mu Z^\mu + \frac{m_Z}{v} Z_\mu \left( \rho_1 \partial^\mu \eta_1 - \eta_1 \partial^\mu \rho_1 + \rho_2 \partial^\mu \eta_2 - \eta_2 \partial^\mu \rho_2 \right) \\ & \approx \frac{m_Z^2}{v} \left[ c_{\beta-\alpha} h_1 + s_{\beta-\alpha} h_2 - (\varepsilon_1 c_{\beta-\alpha} + \varepsilon_2 s_{\beta-\alpha}) h_4 \right] Z_\mu Z^\mu \\ & + \frac{m_Z^2}{2v^2} \left[ h_1^2 + h_2^2 - 2\varepsilon_1 h_1 h_4 - 2\varepsilon_2 h_2 h_4 \right] Z_\mu Z^\mu \\ & + \frac{N_A m_Z}{v} Z_\mu \left[ s_{\beta-\alpha} (h_1 \partial^\mu h_4 - h_4 \partial^\mu h_1) - c_{\beta-\alpha} (h_2 \partial^\mu h_4 - h_4 \partial^\mu h_2) \right. \\ & \quad \left. + \varepsilon_3 s_{\beta-\alpha} (h_1 \partial^\mu h_3 - h_3 \partial^\mu h_1) - \varepsilon_3 c_{\beta-\alpha} (h_2 \partial^\mu h_3 - h_3 \partial^\mu h_2) \right. \\ & \quad \left. - (c_{\beta-\alpha} \varepsilon_1 - s_{\beta-\alpha} \varepsilon_2) (h_1 \partial^\mu h_2 - h_2 \partial^\mu h_1) \right] + \mathcal{O}(\varepsilon_i^2). \end{aligned} \quad (\text{C.9})$$

## References

- [1] G. C. Branco, P. M. Ferreira, L. Lavoura, M. N. Rebelo, M. Sher and J. P. Silva, Phys. Rept. **516** (2012), 1-102 doi:10.1016/j.physrep.2012.02.002 [[arXiv:1106.0034](#) [hep-ph]].
- [2] R. Aaij *et al.* [LHCb Collaboration], Phys. Rev. Lett. **113** (2014) 151601 [[arXiv:1406.6482](#) [hep-ex]].
- [3] R. Aaij *et al.* [LHCb], Phys. Rev. Lett. **122**, no.19, 191801 (2019) [[arXiv:1903.09252](#) [hep-ex]].
- [4] S. Bifani (2017), Seminar at CERN, <https://indico.cern.ch/event/580620/>; S. Bifani [LHCb Collaboration], [arXiv:1705.02693](#) [hep-ex]; R. Aaij *et al.* [LHCb Collaboration], JHEP **1708** (2017) 055 [[arXiv:1705.05802](#) [hep-ex]].
- [5] R. Aaij *et al.* [LHCb Collaboration], Phys. Rev. Lett. **111** (2013) 191801 [[arXiv:1308.1707](#) [hep-ex]]; R. Aaij *et al.* [LHCb Collaboration], JHEP **1602** (2016) 104 [[arXiv:1512.04442](#) [hep-ex]].
- [6] A. Abdesselam *et al.* [Belle], [arXiv:1904.02440](#) [hep-ex].
- [7] W. Altmannshofer, P. S. B. Dev, A. Soni and Y. Sui, Phys. Rev. D **102**, no.1, 015031 (2020) [[arXiv:2002.12910](#) [hep-ph]].
- [8] J. Aebischer, W. Altmannshofer, D. Guadagnoli, M. Reboud, P. Stangl and D. M. Straub, Eur. Phys. J. C **80** (2020) no.3, 252 [[arXiv:1903.10434](#) [hep-ph]].
- [9] M. Algueró, B. Capdevila, A. Crivellin, S. Descotes-Genon, P. Masjuan, J. Matias, M. Novoa Brunet and J. Virto, Eur. Phys. J. C **79** (2019) no.8, 714 [[arXiv:1903.09578](#) [hep-ph]].

- [10] L. Bian, S. M. Choi, Y. J. Kang and H. M. Lee, Phys. Rev. D **96** (2017) no.7, 075038 [[arXiv:1707.04811](#) [hep-ph]].
- [11] L. Bian, H. M. Lee and C. B. Park, Eur. Phys. J. C **78** (2018) no.4, 306 [[arXiv:1711.08930](#) [hep-ph]].
- [12] A. Abdesselam *et al.*, [arXiv:1908.01848](#) [hep-ex].
- [13] S. Kanemura, M. Kubota and K. Yagyu, [[arXiv:2004.03943](#) [hep-ph]].
- [14] J. P. Lees *et al.* [BaBar Collaboration], Phys. Rev. Lett. **109** (2012) 101802 [[arXiv:1205.5442](#) [hep-ex]]; J. P. Lees *et al.* [BaBar Collaboration], Phys. Rev. D **88** (2013) no.7, 072012 [[arXiv:1303.0571](#) [hep-ex]].
- [15] M. Huschle *et al.* [Belle Collaboration], Phys. Rev. D **92** (2015) no.7, 072014 [[arXiv:1507.03233](#) [hep-ex]]; A. Abdesselam *et al.* [Belle Collaboration], [arXiv:1603.06711](#) [hep-ex].
- [16] A. Abdesselam *et al.* [Belle], [[arXiv:1904.08794](#) [hep-ex]].
- [17] R. Aaij *et al.* [LHCb Collaboration], Phys. Rev. Lett. **115** (2015) no.11, 111803 doi:10.1103/PhysRevLett.115.111803. [[arXiv:1506.08614](#) [hep-ex]]; Erratum: [Phys. Rev. Lett. **115** (2015) no.15, 159901]
- [18] Y. S. Amhis *et al.* [HFLAV], [arXiv:1909.12524](#) [hep-ex].
- [19] G. Caria *et al.* [Belle], Phys. Rev. Lett. **124** (2020) no.16, 161803 [[arXiv:1910.05864](#) [hep-ex]].
- [20] S. M. Choi, Y. J. Kang, H. M. Lee and T. G. Ro, JHEP **10** (2018), 104 [[arXiv:1807.06547](#) [hep-ph]].
- [21] B. C. Allanach, J. M. Butterworth and T. Corbett, JHEP **08** (2019), 106 [[arXiv:1904.10954](#) [hep-ph]].
- [22] V. Andreev *et al.* [ACME Collaboration], Nature **562** (2018) no.7727, 355.
- [23] S. M. Barr and A. Zee, Phys. Rev. Lett. **65**, 21 (1990) Erratum: [Phys. Rev. Lett. **65**, 2920 (1990)].
- [24] D. Chang, W. Y. Keung and T. C. Yuan, Phys. Rev. D **43**, 14 (1991).
- [25] R. G. Leigh, S. Paban and R. M. Xu, Nucl. Phys. B **352**, 45 (1991).
- [26] T. Abe, J. Hisano, T. Kitahara and K. Tobioka, JHEP **1401**, 106 (2014) Erratum: [JHEP **1604**, 161 (2016)] [[arXiv:1311.4704](#) [hep-ph]].
- [27] J. Shu and Y. Zhang, Phys. Rev. Lett. **111** (2013) no.9, 091801 [[arXiv:1304.0773](#) [hep-ph]].

- [28] L. Bian, T. Liu and J. Shu, Phys. Rev. Lett. **115** (2015), 021801 [[arXiv:1411.6695](#) [hep-ph]].
- [29] L. Bian and N. Chen, Phys. Rev. D **95** (2017) no.11, 115029 [[arXiv:1608.07975](#) [hep-ph]].
- [30] L. Bian, N. Chen and Y. Zhang, Phys. Rev. D **96** (2017) no.9, 095008 [[arXiv:1706.09425](#) [hep-ph]].
- [31] G. W. Bennett *et al.* [Muon g-2 Collaboration], Phys. Rev. D **73** (2006) 072003 [[hep-ex/0602035](#)].
- [32] C. Patrignani *et al.* [Particle Data Group], Chin. Phys. C **40** (2016) no.10, 100001.
- [33] T. Aoyama *et al.*, [arXiv:2006.04822](#) [hep-ph].
- [34] D. Hanneke, S. Fogwell and G. Gabrielse, Phys. Rev. Lett. **100** (2008) 120801 [[arXiv:0801.1134](#) [physics.atom-ph]]; D. Hanneke, S. F. Hoogerheide and G. Gabrielse, Phys. Rev. A **83** (2011) 052122 [[arXiv:1009.4831](#) [physics.atom-ph]].
- [35] F. Jegerlehner, Acta Phys. Polon. B **49** (2018) 1157 [[arXiv:1804.07409](#) [hep-ph]]; H. Davoudiasl and W. J. Marciano, Phys. Rev. D **98** (2018) no.7, 075011 [[arXiv:1806.10252](#) [hep-ph]]; J. Liu, C. E. M. Wagner and X. P. Wang, JHEP **1903** (2019) 008 [[arXiv:1810.11028](#) [hep-ph]].
- [36] C. Y. Chen, S. Dawson and Y. Zhang, JHEP **06** (2015), 056 [[arXiv:1503.01114](#) [hep-ph]].
- [37] S. Inoue, M. J. Ramsey-Musolf and Y. Zhang, Phys. Rev. D **89** (2014) 11, 115023 [[arXiv:1403.4257](#) [hep-ph]].
- [38] D. Bowser-Chao, D. Chang and W. Y. Keung, Phys. Rev. Lett. **79**, 1988 (1997) [[hep-ph/9703435](#)].
- [39] V. Ilisie, [arXiv:1502.04199](#) [hep-ph].
- [40] U. Haisch and G. Polesello, JHEP **09**, 151 (2018) [[arXiv:1807.07734](#) [hep-ph]].
- [41] F. Kling, H. Li, A. Pyarelal, H. Song and S. Su, JHEP **06**, 031 (2019) [[arXiv:1812.01633](#) [hep-ph]].
- [42] H. E. Haber and A. Pomarol, Phys. Lett. B **302**, 435-441 (1993) [[arXiv:hep-ph/9207267](#) [hep-ph]].
- [43] A. Pomarol and R. Vega, Nucl. Phys. B **413**, 3-15 (1994) [[arXiv:hep-ph/9305272](#) [hep-ph]].
- [44] J. M. Gerard and M. Herquet, Phys. Rev. Lett. **98**, 251802 (2007) [[arXiv:hep-ph/0703051](#) [hep-ph]].

- [45] B. Grzadkowski, M. Maniatis and J. Wudka, JHEP **11**, 030 (2011) [[arXiv:1011.5228](#) [hep-ph]].
- [46] H. E. Haber and D. O’Neil, Phys. Rev. D **83**, 055017 (2011) [[arXiv:1011.6188](#) [hep-ph]].
- [47] F. Kling, S. Su and W. Su, JHEP **06**, 163 (2020) [[arXiv:2004.04172](#) [hep-ph]].
- [48] M. Aaboud *et al.* [ATLAS], JHEP **03**, 174 (2018) [[arXiv:1712.06518](#) [hep-ex]].
- [49] M. Aaboud *et al.* [ATLAS], Phys. Lett. B **783**, 392-414 (2018) [[arXiv:1804.01126](#) [hep-ex]].
- [50] A. M. Sirunyan *et al.* [CMS], Eur. Phys. J. C **79**, no.7, 564 (2019) [[arXiv:1903.00941](#) [hep-ex]].
- [51] A. M. Sirunyan *et al.* [CMS], JHEP **03**, 065 (2020) [[arXiv:1910.11634](#) [hep-ex]].
- [52] D. A. Demir and L. Everett, Phys. Rev. D **69** (2004), 015008 [[arXiv:hep-ph/0306240](#) [hep-ph]].
- [53] L. Bian, H. K. Guo and J. Shu, Chin. Phys. C **42** (2018) no.9, 093106 [[arXiv:1704.02488](#) [hep-ph]].
- [54] R. Zhou and L. Bian, [[arXiv:2001.01237](#) [hep-ph]].
- [55] G. C. Dorsch, S. J. Huber, T. Konstandin and J. M. No, JCAP **05** (2017), 052 doi:10.1088/1475-7516/2017/05/052 [[arXiv:1611.05874](#) [hep-ph]].